

Angiotensin II Induces a Region-Specific Hyperplasia of the Ascending Aorta Through Regulation of Inhibitor of Differentiation 3

A. Phillip Owens, III, Venkateswaran Subramanian, Jessica J. Moorleghen, Zhenheng Guo, Coleen A. McNamara, Lisa A. Cassis and Alan Daugherty

Circ. Res. 2010;106;611-619; originally published online Dec 17, 2009;

DOI: 10.1161/CIRCRESAHA.109.212837

Circulation Research is published by the American Heart Association, 7272 Greenville Avenue, Dallas, TX 75214

Copyright © 2010 American Heart Association. All rights reserved. Print ISSN: 0009-7330. Online ISSN: 1524-4571

The online version of this article, along with updated information and services, is located on the World Wide Web at:

<http://circres.ahajournals.org/cgi/content/full/106/3/611>

Data Supplement (unedited) at:

<http://circres.ahajournals.org/cgi/content/full/CIRCRESAHA.109.212837/DC1>

Subscriptions: Information about subscribing to Circulation Research is online at
<http://circres.ahajournals.org/subscriptions/>

Permissions: Permissions & Rights Desk, Lippincott Williams & Wilkins, a division of Wolters Kluwer Health, 351 West Camden Street, Baltimore, MD 21202-2436. Phone: 410-528-4050. Fax: 410-528-8550. E-mail:
journalpermissions@lww.com

Reprints: Information about reprints can be found online at
<http://www.lww.com/reprints>

Angiotensin II Induces a Region-Specific Hyperplasia of the Ascending Aorta Through Regulation of Inhibitor of Differentiation 3

A. Phillip Owens III, Venkateswaran Subramanian, Jessica J. Moorleghen, Zhenheng Guo, Coleen A. McNamara, Lisa A. Cassis, Alan Daugherty

Rationale: Angiotensin II (Ang II) has diverse effects on smooth muscle cells (SMCs). The diversity of effects may relate to the regional location of this cell type.

Objective: The aim of this study was to define whether Ang II exerted divergent effects on smooth muscle cells in the aorta and determine the role of blood pressure and specific oxidant mechanisms.

Methods and Results: Ang II (1000 ng/kg per minute) infusion for 28 days into mice increased systolic blood pressure and promoted medial expansion of equivalent magnitude throughout the entire aorta. Both effects were ablated by angiotensin II type 1a (AT_{1a}) receptor deficiency. Similar increases in systolic blood pressure by administration of norepinephrine promoted no changes in aortic medial thickness. Increased medial thickness was attributable to SMC expansion owing to hypertrophy in most aortic regions, with the exception of hyperplasia of the ascending aorta. Deficiency of the p47^{phox} component of NADPH oxidase ablated Ang II-induced medial expansion in all aortic regions. Analysis of mRNA and protein throughout the aorta revealed a much higher abundance of the inhibitor of differentiation 3 (Id3) in the ascending aorta compared to all other regions. A functional role was demonstrated by Id3 deficiency inhibiting Ang II-induced SMC hyperplasia of the ascending aorta.

Conclusions: In conclusion, Ang II promotes both aortic medial hypertrophy and hyperplasia in a region-specific manner via an oxidant mechanism. The ascending aortic hyperplasia is dependent on Id3. (*Circ Res.* 2010;106:611-619.)

Key Words: angiotensin II ■ hypertrophy ■ hyperplasia ■ p47^{phox} ■ Id3

Angiotensin II (Ang II) has many physiological and pathological effects on smooth muscle cells (SMCs) of aortic tissue both in vitro and in vivo. Most studies on cultured aortic SMCs have isolated cells from the thoracic region of rats.¹⁻³ In these cells, Ang II consistently promotes hypertrophy,^{1,2} with a lesser number of studies demonstrating a proliferation response.³ The relative effects of Ang II on hypertrophy versus proliferation, in vitro, appear to depend on culture conditions, such as confluence and the coincubation with specific cytokines.³ The expression of the cyclin-dependent kinase inhibitor p27^{kip1}, in cultured cells, is a factor determining the relative effect on hypertrophy versus proliferation.⁴

Many Ang II-induced responses on SMCs are attributable to stimulation of NADPH oxidase with the subsequent generation of reactive oxygen species (ROS).⁵⁻⁷ These include Ang II-induced hypertrophy and proliferative re-

sponses. NADPH oxidase is a multimeric complex. SMCs express specific isoforms of gp91^{phox}, with nox1 being the principal regulator of Ang II-induced responses.⁸⁻¹⁰ The activity of nox1 is regulated by the presence of p47^{phox}.¹¹ Consistent with the nox1-p47^{phox} axis, deficiency of p47^{phox} blunts Ang II-induced increases in systolic blood pressure (SBP).¹² More recently, the dominant-negative helix-loop-helix, inhibitor of differentiation 3 (Id3), has been invoked as a regulator of redox-mediated Ang II induced proliferation.^{13,14}

Ang II effects on aortic contractile responses have provided insight that this octapeptide has region-specific effects. Ang II does not induce contractions of mouse aortic rings isolated from thoracic tissue, but generates a large transient contraction in abdominal tissue in vitro.^{15,16} Contractions of aortic rings are mediated by angiotensin II type 1b (AT_{1b}) receptors despite the presence of AT_{1a} receptors, which may

Original received February 15, 2008; first resubmission received January 13, 2009; second resubmission received November 13, 2009; revised second resubmission received December 9, 2009; accepted December 9, 2009.

From the Saha Cardiovascular Research Center (A.P.O., V.S., J.J.M., Z.G., A.D.); and Graduate Center for Nutritional Sciences (L.A.C., A.D.), University of Kentucky, Lexington; and Department of Internal Medicine (C.A.M.), Cardiovascular Division; and Cardiovascular Research Center, University of Virginia, Charlottesville.

This manuscript was sent to Kathy Griendling, Consulting Editor, for review by expert referees, editorial decision, and final disposition.

Correspondence to Alan Daugherty, Saha Cardiovascular Research Center, BBSRB, room B-243, University of Kentucky, Lexington, KY 40536-0509. E-mail Alan.Daugherty@uky.edu

© 2010 American Heart Association, Inc.

Circulation Research is available at <http://circres.ahajournals.org>

DOI: 10.1161/CIRCRESAHA.109.212837

Non-standard Abbreviations and Acronyms

Ang II	angiotensin II
AT₁	angiotensin II type 1
Id3	inhibitor of differentiation 3
NE	norepinephrine
ROS	reactive oxygen species
SBP	systolic blood pressure
SMC	smooth muscle cell

be indicative of divergent signaling mechanisms stimulated by these subtypes.^{15,16} Region-specific effects on aorta have been noted in response to other bioactivators such as transforming growth factor- β .^{17,18} These region-specific effects may be attributable to the phenotypic diversity of aortic SMCs that arise as a consequence of heterogeneity of embryological origin.¹⁹

Ang II infusion, *in vivo*, is well known to promote changes in medial aortic SMCs via mechanisms that are independent of increased systolic blood pressure.²⁰ The aim of the present study was to determine whether Ang II infusion *in vivo* promoted heterogeneous effects on SMC growth and/or proliferation throughout the entire aorta. Despite previously described differences in contractile activity of Ang II on thoracic versus abdominal aorta,^{15,16} we were unable to demonstrate morphological differences in these two regions during Ang II infusion. However, the ascending aorta has a different response than the rest of the aorta with a medial expansion that was attributable to hyperplasia, versus hypertrophy in other regions. Aortic medial expansion throughout the aorta was ablated by deficiency of p47^{phox}, whereas deficiency of Id3 inhibited the hyperplasia induced by Ang II in the ascending aorta.

Methods

AT_{1a} receptor-deficient (B.129P2-Agtr1a^{tm1UNC}), C57BL/6, and p47^{phox} mutant [B6(Cg)-Ncf1^{m11/J}, C57^{p47/p47}] mice were purchased from The Jackson Laboratory. Id3-deficient mice were a generous gift from Dr Zhang (Duke University). All studies were conducted using male mice with littermate controls.

An expanded Methods section is available in the Online Data Supplement at <http://circres.ahajournals.org>.

Results

Ang II Infusion Uniformly Increased Aortic Thickening via AT_{1a} Receptors, Independent of Pressure

Ang II infusion (1000 ng/kg per minute) into C57BL/6 mice led to a sustained increase in SBP (≈ 40 mm Hg) during the 28 days of delivery (Figure 1A). Ang II infusion also led to increased medial thickness and area to a similar percent in all aortic regions (Figure 1B and Online Table I). To determine the contribution of pressure per se to medial expansion, norepinephrine (NE) was administered to male C57BL/6 mice at doses that increased systolic blood pressure by the same magnitude as Ang II (approximately 40 to 50 mm Hg).

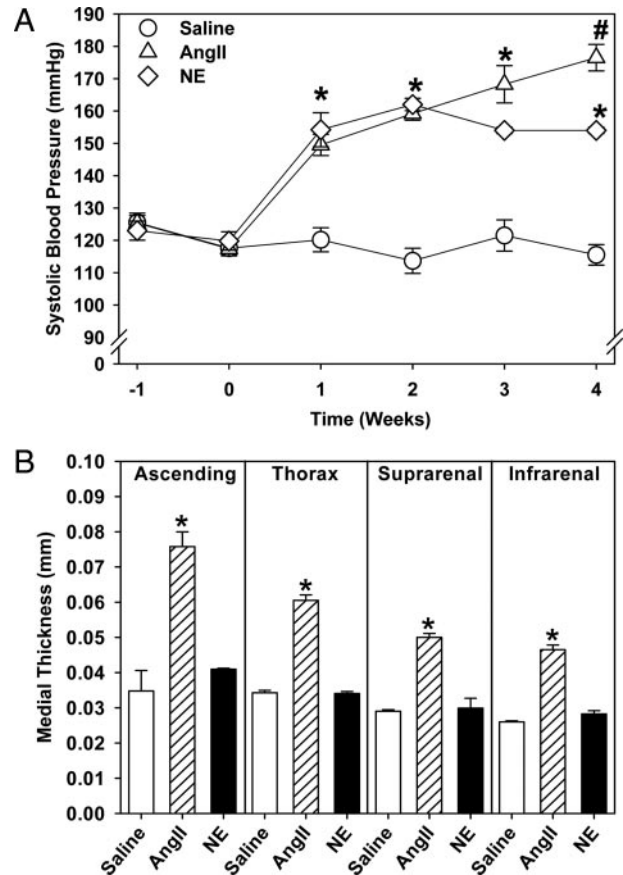


Figure 1. Ang II induced uniform medial expansion throughout the aorta independent of increased SBP. A, SBP was measured before pump implantation and every week during drug administration. Points represent the mean of weekly observations ($n=5$), and bars represent SEM. * $P<0.0001$, Ang II and NE vs saline using repeated measures with Bonferroni post hoc. # $P<0.003$, Ang II vs NE at week 4. B, Aortic medial thickness measured in arch, thoracic, supra-, and infrarenal sections of aorta from C57BL/6 mice infused with saline, Ang II, or NE. Histograms are means of 5 to 10 mice \pm SEM. * $P<0.001$, Ang II-infused mice vs the other 2 groups (1-way ANOVA with Holm-Sidak post hoc).

Contrary to Ang II infusion, NE administration led to no significant changes in medial thickness compared to age-, gender-, and strain-matched mice infused with saline. Equivalent data were also obtained by increasing blood pressure through administration of *N*^ω-nitro-L-arginine methyl ester (data not shown).

To define whether Ang II-induced medial thickening was mediated through AT_{1a} receptors, similar experiments were performed in AT_{1a} receptor^{-/-} mice. Plasma renin concentrations were markedly increased in saline-infused AT_{1a} receptor^{-/-} mice compared to C57BL/6 wild type controls (Online Table I). Interestingly, Ang II infusion reduced plasma renin concentrations in both C57BL/6 and AT_{1a} receptor^{-/-} mice. To determine whether AT_{1b} receptors mediated effects of Ang II to reduce plasma renin concentrations in AT_{1a} receptor^{-/-} mice, we coinfused Ang II and losartan. Ang II-mediated reductions in plasma renin concentrations were abolished in AT_{1a} receptor^{-/-} mice administered losartan. Ang II infusion failed to change SBP in AT_{1a}

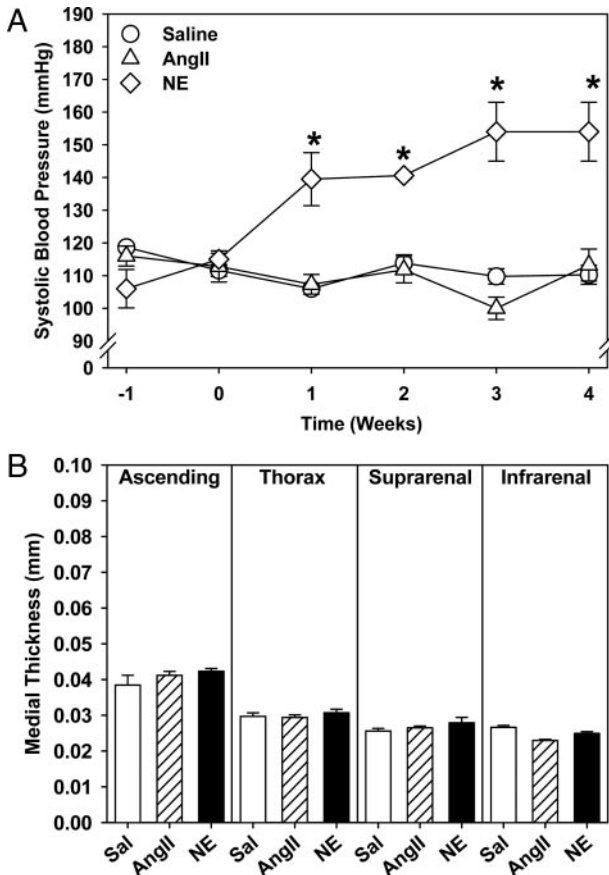


Figure 2. Ang II infusion induced medial thickening via interaction with AT_{1a} receptors. A, SBP was measured before pump implantation and every week during drug administration in AT_{1a} receptor $^{-/-}$ mice. Points represent the mean of weekly observations ($n=5$) and bars represent SEM. $*P<0.0001$, NE vs saline or Ang II using repeated measures with Bonferroni post hoc. B, Aortic medial thickness measured in arch, thoracic, supra-, and infra-renal sections of aorta from AT_{1a} receptor $^{-/-}$ mice. Histograms represent means \pm SEM.

receptor $^{-/-}$ mice (Figure 2A). Moreover, infusion of Ang II did not change aortic medial thickness or area in AT_{1a} receptor $^{-/-}$ mice (Figure 2B and Online Table I). Infusion of NE increased SBP in AT_{1a} receptor $^{-/-}$ mice (Figure 2A). However, NE infusion had no effect on plasma renin concentrations or medial dimensions in any aortic region of AT_{1a} receptor $^{-/-}$ mice (Figure 2B and Online Table I).

The Basis of Ang II–Induced Medial Thickening Differed Among Aortic Regions

Medial thickening with Ang II infusion was associated with a marked expansion of the intralaminar space in all aortic regions (Figure 3). This expansion may potentially be attributable to contributions from extracellular matrix expansion, and SMC hypertrophy or hyperplasia. To determine the contribution of extracellular matrix, aortas were stained with Movat's pentachrome to permit visualization of elastin, collagen, and proteoglycans (Online Figure III). There were no overt differences in staining for extracellular matrix components. Serial sections from all regions were immunostained for α -actin or stained with

propidium iodide to access expansion of cell size and number, respectively (Figure 3). Immunostaining for α -actin demonstrated uniform reactivity throughout the intra laminar spaces (Figure 3A). Nuclei counts were normalized to a standard section length, because the medial expansion confounded the utilization of vessel area. Ang II infusion did not significantly affect nuclei density in both thoracic and abdominal aortic regions (Figure 3B). When combined with data from immunostaining, this was consistent, with the medial expansion being attributable to increased volume of SMCs. Unexpectedly, Ang II promoted a marked increase in nuclei density in tissue sections from the ascending aorta (Figure 3B). Because this entire region immunostained positively for SMCs, this was consistent with medial expansion caused by hyperplasia. Ang II also exerted region-specific effects on cultured SMCs. In agreement with the observations in vivo, Ang II promoted a proliferation of SMCs cultured from ascending aortas, but not in SMCs isolated from other aortic regions (Online Figure IV). Platelet-derived growth factor-BB promoted similar proliferation in SMCs cultured from all aortic regions. Therefore, the basis for Ang II–induced medial expansion differed among aortic regions.

Ang II–Induced Growth Suppression Is Unchanged Among Aortic Regions

The previous data demonstrate Ang II induction of vascular growth and proliferation. However, Ang II can also act as a potent growth suppressor. Therefore, we evaluated apoptotic events via TUNEL. SMCs cultured from different aortic regions significantly increased apoptotic events with the addition of Ang II versus saline (≈ 10 -fold); however, there was no difference between the four regions (Online Figure V). These data do not support differences in Ang II–induced growth suppression among the aortic regions.

p47^{phox} Deficiency Ablated Ang II–Induced Medial Thickness

Given the role of Ang II–induced ROS on SMC hypertrophy and hyperplasia, and the above region-specific data, we examined whether concentrations of superoxide (O_2^-) and hydrogen peroxide (H_2O_2) differed along the aorta. In SMCs cultured from different aortic regions, there was uniform expression of ROS in all aortic regions examined (Online Figure VI). Furthermore, in vivo and ex vivo measurement of aortic O_2^- demonstrated no regional differences throughout the aorta (Online Figure VII). To determine whether inability to generate ROS resulted in functional changes in vivo, saline, Ang II, or NE was infused into mice with a spontaneous loss of functional mutation for p47^{phox}. Basal blood pressure was not different between p47^{phox}-deficient mice compared to wild type (C57BL/6). Ang II infusion did not increase blood pressure initially in p47^{phox} functionally deficient mice (Figure 4), but did result in a belated increase during week 4 of infusion. Plasma renin concentrations were unchanged in saline-infused p47^{phox}-deficient compared to wild type mice, and infusion of Ang II led to similar reductions in

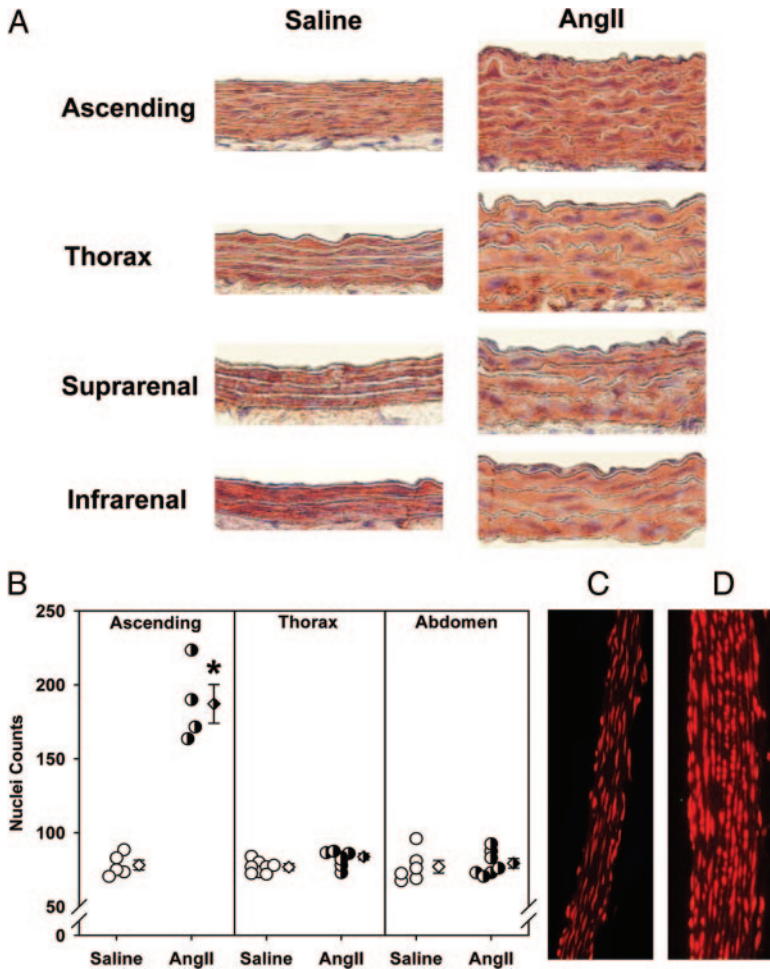


Figure 3. Ang II infusion induced medial thickness by either hypertrophy or hyperplasia. A, Representative C57BL/6 aortic sections immunostained for α -actin. Tissue sections from ascending, thoracic, suprarenal, and infrarenal aortas of mice infused with either saline or Ang II for 28 days were immunostained with a rabbit anti- α -actin (1:200 dilution). B, Nuclei density are represented by normalization to aortic section length (0.25 mm). Circles represent means of individual mice; diamonds, means of 5 to 10 mice in each group \pm SEM. * $P < 0.001$, differences between saline and Ang II-infused mice using a Student *t* test. Examples of aortic arch sections from mice infused with saline (C) or Ang II (D) and stained with propidium iodide.

plasma renin concentrations in p47^{phox}-deficient mice (Online Table I). The functional deficiency of p47^{phox} had no effect on the ability of NE infusion to increase SBP (Figure 4A). The absence of functional p47^{phox} abolished Ang II-induced increases in medial thickness for all regions of the aorta (Figure 4B).

Ang II Initiated Id3 Translocation to Nuclei

To provide a basis for Ang II-induced medial SMC hyperplastic response that was limited to the ascending portion of aortas, we defined the expression of Id3. Real-time PCR analysis of Id3 mRNA demonstrated significantly increased (3.5 fold) abundance in ascending aortas versus other aortic regions (Figure 5A). Western blotting of Id3 protein in cultured SMCs revealed similar regional differences in the aorta (Figure 5B through 5D; Online Figure VIII). As noted previously,²¹ Id3 abundance fluctuated over time in the presence of serum, but was always greater in cells isolated from the ascending region. Furthermore, Ang II incubation of SMCs isolated from ascending aortas resulted in Id3 colocalization within nuclei at 1 and 24 hours, with cycling to the cytoplasmic compartment at 12 hours (Online Figures IX through XI). This effect was not observed in other aortic regions (Online Figure XI). These data demonstrate Ang II initiates cyclic Id3 localization to the nuclei compartment of SMC in the ascending aorta, suggesting novel mechanisms

whereby Id3 mediates the regional hyperplastic effects of Ang II.

Id3 Deficiency Ablated Ascending Aortic Hyperplasia

To determine the in vivo contribution of Id3 to Ang II-induced ascending aortic hyperplasia, Id3^{-/-} mice were infused with either saline or Ang II. Ang II markedly increased SBP in Id3^{-/-} mice (Figure 6A). Furthermore, Id3 deficiency did not abolish Ang II-induced increases of medial thickness in the ascending and abdominal regions (Figure 6B). Similar to Id3^{+/+} mice, immunostaining of aortas from Id3^{-/-} mice with α -actin demonstrated uniform reactivity throughout the intralaminar spaces and no overt matrix deposition by Movat's pentachrome staining (data not shown). Moreover, plasma renin concentrations were similarly reduced by Ang II infusion in Id3^{-/-} mice, compared to other mouse strains (Online Table I). SMC nuclei density was unchanged in other aortic regions compared to wild type mice (data not shown). However, Ang II-induced increases in ascending aortic SMC nuclei density were strikingly reduced by Id3 deficiency (Figure 7).

Discussion

This study demonstrated that Ang II promoted a uniform medial expansion throughout the aorta. Despite the unifor-

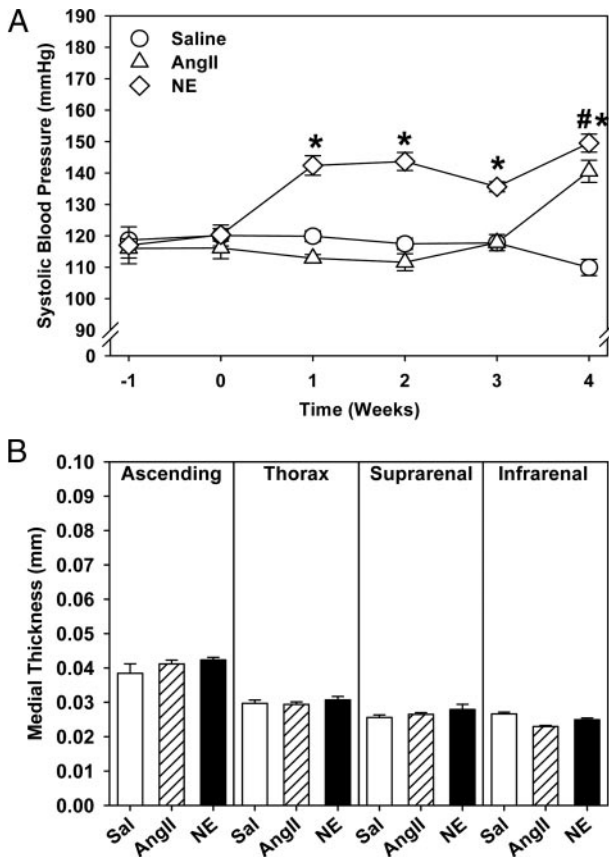


Figure 4. Functional deficiency of p47^{phox} attenuated both Ang II-induced hypertrophy and hyperplasia. A, SBP was measured before pump implantation and every week during infusion with saline, Ang II, or NE. Points represent means of weekly observations (n=5), and bars represent SEM. **P*<0.0001, NE vs saline or Ang II using repeated measures with Bonferroni post hoc. #*P*<0.01, Ang II vs saline infused mice. B, Effects of infusions on medial thickness in p47^{phox}-deficient mice in 4 aortic regions. Histograms are means of 5 mice±SEM.

mity of the expansion, the underlying cause differed in a region-specific manner. SMC hyperplasia occurred in the ascending aorta, but SMC's hypertrophied in all other aortic regions. This effect was attributable to stimulation of AT_{1a} receptors, but independent of increases in SBP. Ang II-induced medial expansion was ablated in all aortic regions in mice with functional deficiency of p47^{phox}, whereas the hyperplastic response localized to the ascending aorta was inhibited by deficiency of Id3.

Ang II-induced medial expansion has the potential to be attributable to both cellular and extracellular components. Although Ang II is known to increase several extracellular matrix proteins, including collagen^{22,23} and proteoglycans,²⁴ these did not appear to provide a major contribution to medial expansion. Therefore, this study focused on the contributions of increases in cellular components to medial expansion. Many studies have demonstrated that Ang II promotes hypertrophy^{1,2} of cultured aortic SMCs, with a lesser number demonstrating proliferation.³ Most of these studies have been performed with SMCs that have been derived from rat thoracic aorta. A lesser number of studies have chronically infused Ang II in vivo to determine

effects on medial dimensions.^{25–27} SMC proliferative responses to Ang II infusion have been demonstrated in rat carotid and mesenteric arteries.^{20,28–30} In contrast, the predominance of studies have demonstrated Ang II increased medial thickness in vivo through hypertrophy of rat^{25,26,28} and mouse^{10,27,31} aortas. The location of aortic sections used in these studies has not been commonly stated, but is likely to be the thoracic region. Thus, the description of medial expansion being attributable to hypertrophy in the thoracic aorta is consistent with the present study. Our results are the first to describe heterogeneity of Ang II-induced responses within the aorta. Results from this study demonstrated that Ang II-induced proliferation was limited to SMCs cultured from the ascending aorta versus other aortic regions. However, the present study did not discern whether the in vivo increase in nuclei was attributable to proliferation or polyploidization, although the magnitude of the increase in nuclei in the ascending aorta is much larger than has been described for polyploidization.^{25,32–34}

The basis for the heterogeneous cause of Ang II-induced medial expansion in different regions of the aorta may be attributable to the diversity of embryonic origin of SMCs with potential functional differences.¹⁹ SMCs in the ascending aortic regions are primarily of neural crest origin, which extends from the aortic root to just distal of the subclavian artery.³⁵ This same lineage also extends to the carotid arteries. Conversely, thoracic and abdominal aortic SMCs are derived from somite and splanchnic mesoderm lineages, respectively. Regional differences in aortic SMCs have been described previously.¹⁹

Deficiency of AT_{1a} receptors ablated Ang II-induced medial expansion in all regions. Previous studies have highlighted the role of the AT_{1b} receptor subtype in aortic function.^{15,36} Although both a and b subtypes of AT₁ receptors are expressed in the mouse aorta, deficiency of the b subtype substantially reduced Ang II-induced contractions that are restricted to the abdominal aorta.¹⁶ Although the 2 subtypes are highly homologous, the differences are predominantly in the final intracellular loop and the cytoplasmic tail of this seven membrane spanning protein.³⁷ These amino acid substitutions have predictive differences on intracellular signaling.^{38,39} Thus, in future studies, the relative differences between the subtypes will provide insight into the definition of the intracellular pathway that leads to medial expansion.

As with previous studies, absence of AT_{1a} receptors had no effect on basal SBP in mice on a C57BL/6 background.^{40–42} Moreover, AT_{1a} receptor deficiency increased plasma renin concentrations, demonstrating removal of Ang II-mediated negative feedback on renin synthesis and secretion.⁴³ This maintenance of pressure is probably attributable to the continued presence of AT_{1b} receptors, because compound deficiency of both subtypes promotes a severe phenotype as occurs with deficiency of angiotensinogen, renin, or angiotensin-converting enzyme.⁴³ The presence of functional AT_{1b} receptors can be inferred in the present study by the down-regulation of plasma renin concentrations during Ang II infusion into AT_{1a} receptor-deficient mice and its reversal

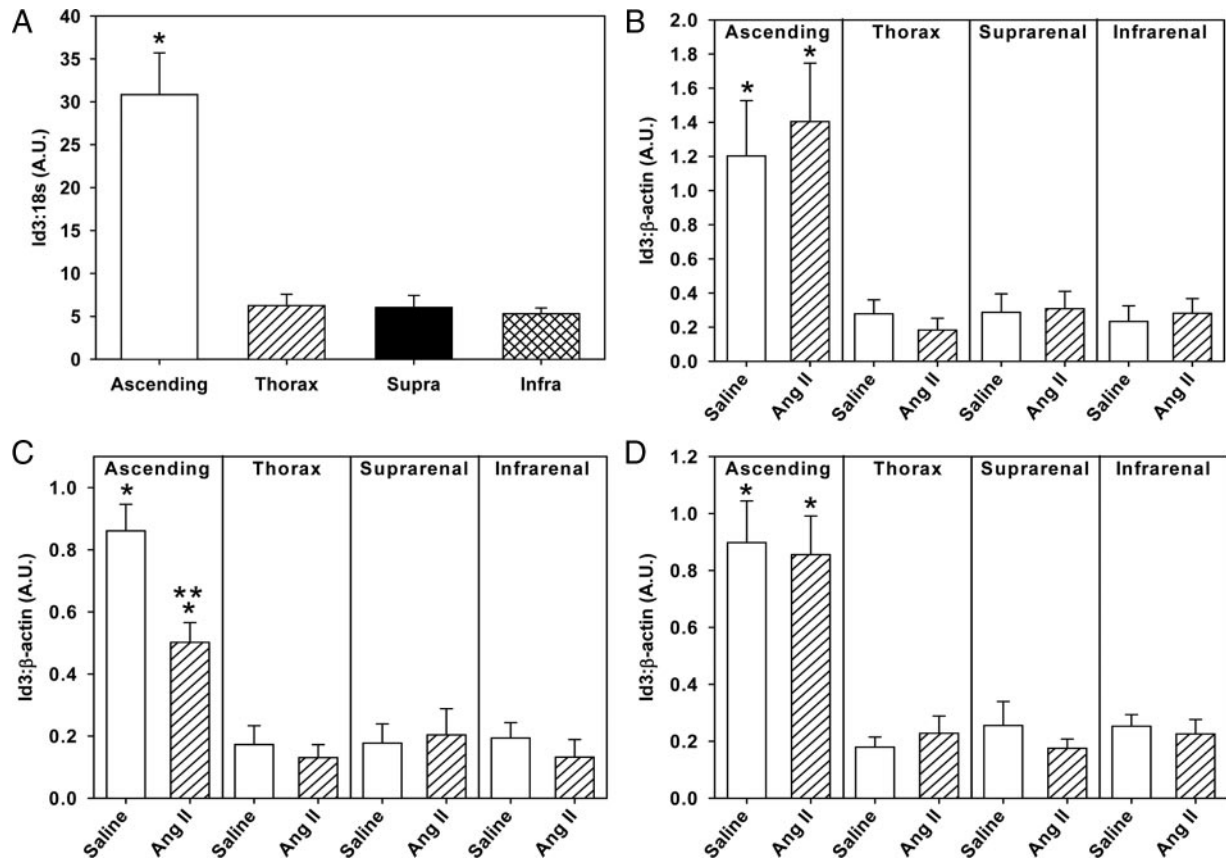


Figure 5. Id3 was most abundant in SMCs of the ascending aortic region. A, Id3 mRNA abundance was quantified by real-time PCR. Histograms are means of 3 mice and bars are SEM. * $P < 0.001$, abundance in ascending aorta vs all other regions (1-way ANOVA). Ascending, thoracic, suprarenal, or infrarenal SMCs were serum-starved for 72 hours and incubated with either saline or Ang II ($1 \mu\text{mol/L}$) for 1 (B), 12 (C), or 24 (D) hours. Histograms represent Id3 protein abundance normalized to β -actin and are means of 5 individual experiments \pm SEM. * $P < 0.001$, ascending aortic SMCs vs all other regions; ** $P < 0.05$, ascending aortic SMCs incubated with Ang II vs saline at the 12-hour interval (1-way ANOVA with Holm-Sidak post hoc).

during concomitant infusion of the AT_1 receptor antagonist losartan.

Numerous studies have demonstrated a functional role of ROS, specifically O_2^- and H_2O_2 , in both hypertrophic and hyperplastic responses of SMCs.^{13,14,31,44} Ang II-induced production of O_2^- and H_2O_2 has the potential to increase redox signaling pathways. However, we were unable to demonstrate any regional differences in ROS production. A major source of ROS during Ang II stimulation of SMCs is via augmentation of NADPH oxidase activity as demonstrated by studies in cultured SMCs^{5,43,45} and in vivo.^{10,27,31} NADPH oxidases are multimeric complexes with components that differ in a cell-specific manner. In regard to Ang II-induced responses in SMCs, these are mediated by a complex containing Nox1 in which p47^{phox} is a critical component for activation.¹¹ The importance of this coupling has been shown using gp91ds-tat, which is a peptide that inhibits the assembly of Nox1 with p47^{phox}.⁴⁶ Gp91ds-tat inhibits Ang II-induced increases in SBP and medial expansion of carotid arteries. Conversely, deficiency of p47^{phox} attenuates Ang II-induced increases in SBP.^{12,47} In contrast to results from the present study, a previous study demonstrated that p47^{phox} deficiency increased basal blood pressure, even though Ang II-induced increases in SBP were attenu-

ated.⁴⁸ Moreover, p47^{phox}-deficient mice showed basal increases in renin,⁴⁸ which we were not able to demonstrate. Differences in results may arise from the mode of interference with p47^{phox}, because the previous study used genetically engineered p47^{phox}-deficient mice, whereas the present study used p47^{phox}-deficient mice that arose from a spontaneous mutation.⁴⁹ Although the spontaneous and engineered mutations are on exon 8 and 7, respectively, there is no obvious basis for these mice exhibiting different manifestations of deficiency. In contrast to the spontaneous mutation, engineered p47^{phox}-deficient mice have been shown previously to exhibit no change in basal SBP. However, other studies have demonstrated a greater effect on SBP during Ang II infusion than in the present study.^{12,50} This greater efficacy of Ang II-induced increases in SBP may be a consequence of the use of the [Val5] variant of Ang II which has a greater efficacy at stimulating AT_1 receptors compared to the Ang II sequence of human and mouse peptides. Irrespective of these differences among studies, the present study demonstrated that deficiency of p47^{phox} ablated aortic medial expansion in all regions.

Ang II-induced proliferation of cultured SMCs occurs via activation of NADPH oxidase with generation of superoxide production that subsequently induces the ex-

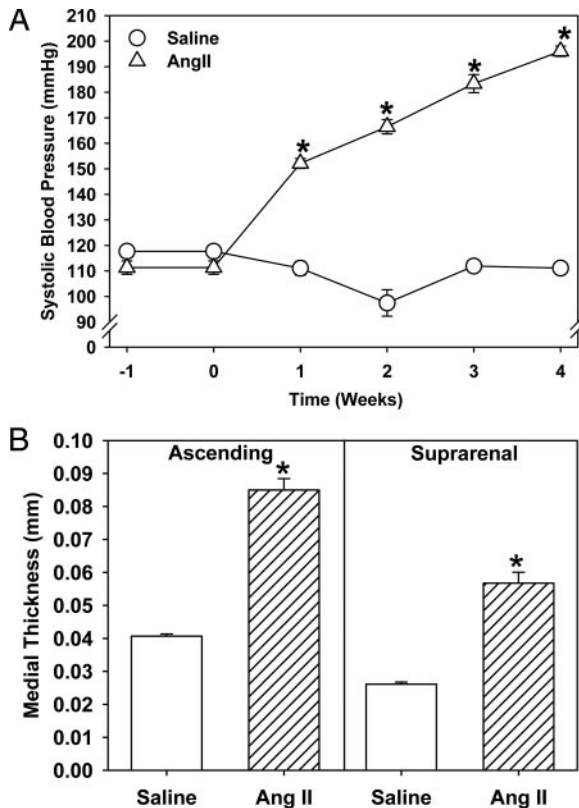


Figure 6. Id3 deficiency did not attenuate Ang II-induced increases in SBP and medial thickness. A, SBP was measured during Ang II infusion in Id3^{-/-} mice. Points represent means of weekly observations \pm SEM (n=5). * $P < 0.0001$, saline vs Ang II-infused mice using repeated measures with Bonferroni post hoc. B, Aortic medial thickness was measured in ascending and suprarenal aortic sections of Id3-deficient mice infused with saline or Ang II. Histograms are means of 6 to 7 mice \pm SEM. * $P < 0.001$, Ang II vs saline infusion (1-way ANOVA with Holm-Sidak post hoc).

pression of the dominant-negative helix-loop-helix protein Id3.^{13,14} Id3 dimerizes with the basic helix-loop-helix factor E47, inhibits E47-induced activation of expression of cyclin dependent kinase inhibitor p21^{WAF1/Cip1}, and promotes SMC proliferation.²¹ This mitotic effect is mediated via nuclei translocation of Id3 from the cytoplasm via an E47 nuclear localization signal.^{51,52} Id3 has also been implicated in proliferative responses to carotid artery injury.⁵³ As noted earlier, the carotid artery shares common embryonic origin with cells of the ascending aorta.^{19,35} In agreement with the disparity of the ascending aorta versus other aortic regions, Id3 mRNA and protein abundance was much greater in this region. In contrast to previous reports using rat thoracic SMCs, in this study Ang II did not upregulate Id3 protein levels in mouse SMCs.¹³ In contrast, we demonstrate that Ang II signaling can initiate Id3 localization to the nuclei compartment at 1 and 24 hours. Previous data demonstrated Id3 was upregulated and phosphorylated at these intervals in correlation with cell cycle progression.²¹ Furthermore, direct evidence of a role of Id3 in the hyperplastic response to Ang II was derived from mice with genetic deficiencies of this protein. Although there is the potential for Id3 deficiency to lead to

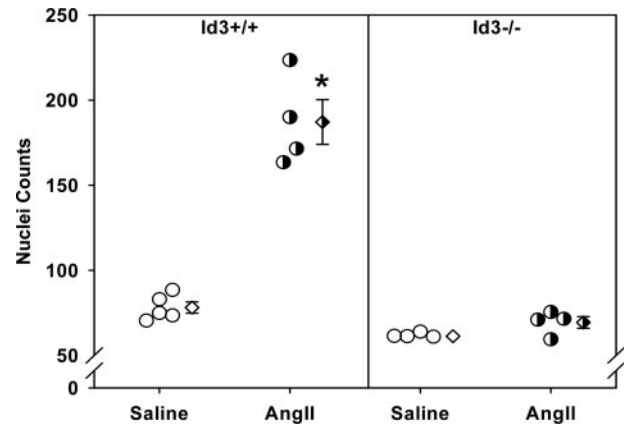


Figure 7. Deficiency of Id3 ablated Ang II-induced hyperplasia in ascending aortas. Nuclei density in ascending aortas from Id3^{+/+} and Id3^{-/-} mice. Circles represent means of individual mice, diamonds represent means of 4 to 5 mice in each group \pm SEM. * $P < 0.001$, ascending aortas from Id3^{+/+} mice infused with Ang II vs saline by Student *t* test.

compensatory increases of other Id proteins, the total ablation of Ang II-induced hyperplasia of the ascending aorta provided a striking demonstration of the specific requirement for Id3. Moreover, effects of Id3 deficiency on Ang II-induced proliferative responses were observed despite a marked increase in the blood pressure response to Ang II, supporting pressure-independent effects of Ang II on SMC proliferation.

In summary, this study demonstrated that Ang II infusion promotes aortic medial expansion by disparate mechanisms in a region-specific manner. A major difference was the demonstration of the disparity of responses in the ascending aorta compared to other regions. Unique responses of this region in aortic luminal expansion have also been demonstrated in mice harboring fibrillin-1 mutations that were infused with Ang II.⁵⁴ Although this study defined Ang II-induced changes in SMCs, this effect could be directly on SMCs or indirectly from another cell type. For example, endothelial cells secrete a wide range of products that directly affect SMC function. Recent data implicate platelet-derived growth factor-DD secretion from endothelial cells as a moderator of SMC phenotypic modulation, particularly in areas of disturbed blood flow such as the aortic arch.⁵⁵ Thus, subsequent studies will determine the contribution of SMC and endothelial cells to the observed phenotypes by using Cre-Lox technology to promote cell-specific AT_{1a} receptor deficiency.

Acknowledgments

We acknowledge the assistance of Victoria English, Deborah A. Howatt, Talha Ijaz, Rohit Malhotra, and Debra L. Rateri.

Sources of Funding

This work was supported by NIH grant HL80100 and an American Heart Association Ohio Valley Affiliate Predoctoral Fellowship (0615222B to A.P.O.).

Disclosures

None.

References

- Owens GK, Rabinovitch PS, Schwartz SM. Smooth muscle cell hypertrophy versus hyperplasia in hypertension. *Proc Natl Acad Sci U S A*. 1981;78:7759–7763.
- Geisterfer AA, Peach MJ, Owens GK. Angiotensin II induces hypertrophy, not hyperplasia, of cultured rat aortic smooth muscle cells. *Circ Res*. 1988;62:749–756.
- Gibbons GH, Pratt RE, Dzau VJ. Vascular smooth muscle cell hypertrophy vs. hyperplasia. Autocrine transforming growth factor-beta 1 expression determines growth response to angiotensin II. *J Clin Invest*. 1992;90:456–461.
- Braun-Dullaeus RC, Mann MJ, Ziegler A, von der Leyen HE, Dzau VJ. A novel role for the cyclin-dependent kinase inhibitor p27(Kip1) in angiotensin II-stimulated vascular smooth muscle cell hypertrophy. *J Clin Invest*. 1999;104:815–823.
- Griendling KK, Minieri CA, Ollerenshaw JD, Alexander RW. Angiotensin II stimulates NADH and NADPH oxidase activity in cultured vascular smooth muscle cells. *Circ Res*. 1994;74:1141–1148.
- Cai H, Griendling KK, Harrison DG. The vascular NAD(P)H oxidases as therapeutic targets in cardiovascular diseases. *Trends Pharmacol Sci*. 2003;24:471–478.
- Mehta PK, Griendling KK. Angiotensin II cell signaling: physiological and pathological effects in the cardiovascular system. *Am J Physiol Cell Physiol*. 2007;292:C82–C97.
- Lassegue B, Sorescu D, Szocs K, Yin Q, Akers M, Zhang Y, Grant SL, Lambeth JD, Griendling KK. Novel gp91(phox) homologues in vascular smooth muscle cells: nox1 mediates angiotensin II-induced superoxide formation and redox-sensitive signaling pathways. *Circ Res*. 2001;88:888–894.
- Hilenski LL, Clempus RE, Quinn MT, Lambeth JD, Griendling KK. Distinct subcellular localizations of Nox1 and Nox4 in vascular smooth muscle cells. *Arterioscler Thromb Vasc Biol*. 2004;24:677–683.
- Dikalova A, Clempus R, Lassegue B, Cheng G, McCoy J, Dikalov S, San Martin A, Lyle A, Weber DS, Weiss D, Taylor WR, Schmidt HH, Owens GK, Lambeth JD, Griendling KK. Nox1 overexpression potentiates angiotensin II-induced hypertension and vascular smooth muscle hypertrophy in transgenic mice. *Circulation*. 2005;112:2668–2676.
- Takeya R, Ueno N, Kami K, Taura M, Kohjima M, Izaki T, Nuno H, Sumimoto H. Novel human homologues of p47phox and p67phox participate in activation of superoxide-producing NADPH oxidases. *J Biol Chem*. 2003;278:25234–25246.
- Landmesser U, Cai H, Dikalov S, McCann L, Hwang J, Jo H, Holland SM, Harrison DG. Role of p47(phox) in vascular oxidative stress and hypertension caused by angiotensin II. *Hypertension*. 2002;40:511–515.
- Mueller C, Baudler S, Welzel H, Bohm M, Nickenig G. Identification of a novel redox-sensitive gene, Id3, which mediates angiotensin II-induced cell growth. *Circulation*. 2002;105:2423–2428.
- Nickenig G, Baudler S, Muller C, Werner C, Werner N, Welzel H, Strehlow K, Bohm M. Redox-sensitive vascular smooth muscle cell proliferation is mediated by GSKF and Id3 in vitro and in vivo. *FASEB J*. 2002;16:1077–1086.
- Zhou Y, Chen Y, Dirksen WP, Morris M, Periasamy M. AT_{1b} receptor predominantly mediates contractions in major mouse blood vessels. *Circ Res*. 2003;93:1089–1094.
- Swafford AN Jr, Harrison-Bernard LM, Dick GM. Knockout mice reveal that the angiotensin II type 1B receptor links to smooth muscle contraction. *Am J Hypertens*. 2007;20:335–337.
- Wrenn RW, Rauber CL, Herman LE, Walton WJ, Rosenquist TH. Transforming growth factor-beta: signal transduction via protein kinase C in cultured embryonic vascular smooth muscle cells. *In Vitro Cell Dev Biol*. 1993;29A:73–78.
- Topouzis S, Majesky MW. Smooth muscle lineage diversity in the chick embryo. Two types of aortic smooth muscle cell differ in growth and receptor-mediated transcriptional responses to transforming growth factor-beta. *Dev Biol*. 1996;178:430–445.
- Majesky MW. Developmental basis of vascular smooth muscle diversity. *Arterioscler Thromb Vasc Biol*. 2007;27:1248–1258.
- Su EJ, Lombardi DM, Siegal J, Schwartz SM. Angiotensin II induces vascular smooth muscle cell replication independent of blood pressure. *Hypertension*. 1998;31:1331–1337.
- Forrest ST, Taylor AM, Sarembok IJ, Perlegas D, McNamara CA. Phosphorylation regulates Id3 function in vascular smooth muscle cells. *Circ Res*. 2004;95:557–559.
- Kato H, Suzuki H, Tajima S, Ogata Y, Tominaga T, Sato A, Saruta T. Angiotensin II stimulates collagen synthesis in cultured vascular smooth muscle cells. *J Hypertens*. 1991;9:17–22.
- Albaladejo P, Bouaziz H, Duriez M, Gohlke P, Levy BI, Safar ME, Benetos A. Angiotensin converting enzyme inhibition prevents the increase in aortic collagen in rats. *Hypertension*. 1994;23:74–82.
- Figueroa JE, Vijayagopal P. Angiotensin II stimulates synthesis of vascular smooth muscle cell proteoglycans with enhanced low density lipoprotein binding properties. *Atherosclerosis*. 2002;162:261–268.
- Owens GK, Schwartz SM. Vascular smooth muscle cell hypertrophy and hyperploidy in the Goldblatt hypertensive rat. *Circ Res*. 1983;53:491–501.
- Owens GK. Influence of blood pressure on development of aortic medial smooth muscle hypertrophy in spontaneously hypertensive rats. *Hypertension*. 1987;9:178–187.
- Weber DS, Rocic P, Mellis AM, Laude K, Lyle AN, Harrison DG, Griendling KK. Angiotensin II-induced hypertrophy is potentiated in mice overexpressing p22phox in vascular smooth muscle. *Am J Physiol Heart Circ Physiol*. 2005;288:H37–H42.
- Owens GK, Schwartz SM, McCanna M. Evaluation of medial hypertrophy in resistance vessels of spontaneously hypertensive rats. *Hypertension*. 1988;11:198–207.
- Wiener J, Lombardi DM, Su JE, Schwartz SM. Immunohistochemical and molecular characterization of the differential response of the rat mesenteric microvasculature to angiotensin-II infusion. *J Vasc Res*. 1996;33:195–208.
- Su EJ, Lombardi DM, Wiener J, Daemen MJ, Reidy MA, Schwartz SM. Mitogenic effect of angiotensin II on rat carotid arteries and type II or III mesenteric microvessels but not type I mesenteric microvessels is mediated by endogenous basic fibroblast growth factor. *Circ Res*. 1998;82:321–327.
- Zhang Y, Griendling KK, Dikalova A, Owens GK, Taylor WR. Vascular hypertrophy in angiotensin II-induced hypertension is mediated by vascular smooth muscle cell-derived H₂O₂. *Hypertension*. 2005;46:732–737.
- Barrett TB, Sampson P, Owens GK, Schwartz SM, Benditt EP. Polyploid nuclei in human artery wall smooth muscle cells. *Proc Natl Acad Sci U S A*. 1983;80:882–885.
- Hixon ML, Muro-Cacho C, Wagner MW, Obejero-Paz C, Millie E, Fujio Y, Kureishi Y, Hassold T, Walsh K, Gualberto A. Akt1/PKB upregulation leads to vascular smooth muscle cell hypertrophy and polyploidization. *J Clin Invest*. 2000;106:1011–1020.
- Hixon ML, Obejero-Paz C, Muro-Cacho C, Wagner MW, Millie E, Nagy J, Hassold TJ, Gualberto A. Cks1 mediates vascular smooth muscle cell polyploidization. *J Biol Chem*. 2000;275:40434–40442.
- Jiang X, Rowitch DH, Soriano P, McMahon AP, Sucov HM. Fate of the mammalian cardiac neural crest. *Development*. 2000;127:1607–1616.
- Zhu Z, Zhang SH, Wagner C, Kurtz A, Maeda N, Coffman T, Arendshorst WJ. Angiotensin AT_{1b} receptor mediates calcium signaling in vascular smooth muscle cells of AT_{1a} receptor-deficient mice. *Hypertension*. 1998;31:1171–1177.
- Sasamura H, Hein L, Krieger JE, Pratt RE, Kobilka BK, Dzau VJ. Cloning, characterization, and expression of two angiotensin receptor (AT-1) isoforms from the mouse genome. *Biochem Biophys Res Commun*. 1992;185:253–259.
- Griendling KK, Lassegue B, Alexander RW. Angiotensin receptors and their therapeutic implications. *Annu Rev Pharmacol Toxicol*. 1996;36:281–306.
- Hein L. Genetic deletion and overexpression of angiotensin II receptors. *J Mol Med*. 1998;76:756–763.
- Mangrum AJ, Gomez RA, Norwood VF. Effects of AT(1A) receptor deletion on blood pressure and sodium excretion during altered dietary salt intake. *Am J Physiol Renal Physiol*. 2002;283:F447–F453.
- Daugherty A, Rateri DL, Lu H, Inagami T, Cassis LA. Hypercholesterolemia stimulates angiotensin peptide synthesis and contributes to atherosclerosis through the AT_{1a} receptor. *Circulation*. 2004;110:3849–3857.
- Cassis LA, Rateri DL, Lu H, Daugherty A. Bone marrow transplantation reveals that recipient AT_{1a} receptors are required to initiate angiotensin II-induced atherosclerosis and aneurysms. *Arterioscler Thromb Vasc Biol*. 2007;27:380–386.

43. Oliverio MI, Kim HS, Ito M, Le T, Audoly L, Best CF, Hiller S, Kluckman K, Maeda N, Smithies O, Coffman TM. Reduced growth, abnormal kidney structure, and type 2 (AT₂) angiotensin receptor-mediated blood pressure regulation in mice lacking both AT_{1A} and AT_{1B} receptors for angiotensin II. *Proc Natl Acad Sci U S A*. 1998;95:15496–15501.
44. Zafari AM, Ushio-Fukai M, Akers M, Yin Q, Shah A, Harrison DG, Taylor WR, Griendling KK. Role of NADH/NADPH oxidase-derived H₂O₂ in angiotensin II-induced vascular hypertrophy. *Hypertension*. 1998;32:488–495.
45. Ushio-Fukai M, Zafari AM, Fukui T, Ishizaka N, Griendling KK. p22phox is a critical component of the superoxide-generating NADH/NADPH oxidase system and regulates angiotensin II-induced hypertrophy in vascular smooth muscle cells. *J Biol Chem*. 1996;271:23317–23321.
46. Liu J, Yang F, Yang XP, Jankowski M, Pagano PJ. NAD(P)H oxidase mediates angiotensin II-induced vascular macrophage infiltration and medial hypertrophy. *Arterioscler Thromb Vasc Biol*. 2003;23:776–782.
47. Thomas M, Gavrilu D, McCormick ML, Miller FJ Jr, Daugherty A, Cassis LA, Dellsperger KC, Weintraub NL. Deletion of p47phox attenuates angiotensin II-induced abdominal aortic aneurysm formation in apolipoprotein E-deficient mice. *Circulation*. 2006;114:404–413.
48. Grote K, Ortmann M, Salguero G, Doerries C, Landmesser U, Luchtefeld M, Brandes RP, Gwinner W, Tschernig T, Brabant EG, Klos A, Schaefer A, Drexler H, Schieffer B. Critical role for p47phox in renin-angiotensin system activation and blood pressure regulation. *Cardiovasc Res*. 2006;71:596–605.
49. Jackson SH, Gallin JI, Holland SM. The p47phox mouse knock-out model of chronic granulomatous disease. *J Exp Med*. 1995;182:751–758.
50. Hsich E, Segal BH, Pagano PJ, Rey FE, Paigen B, Deleonardis J, Hoyt RF, Holland SM, Finkel T. Vascular effects following homozygous disruption of p47(phox): an essential component of NADPH oxidase. *Circulation*. 2000;101:1234–1236.
51. Deed RW, Armitage S, Norton JD. Nuclear localization and regulation of Id protein through an E protein-mediated chaperone mechanism. *J Biol Chem*. 1996;271:23603–23606.
52. O'Toole PJ, Inoue T, Emerson L, Morrison IE, Mackie AR, Cherry RJ, Norton JD. Id proteins negatively regulate basic helix-loop-helix transcription factor function by disrupting subnuclear compartmentalization. *J Biol Chem*. 2003;278:45770–45776.
53. Matsumura ME, Li F, Berthoux L, Wei B, Lobe DR, Jeon C, Hammaraskjold ML, McNamara CA. Vascular injury induces posttranscriptional regulation of the Id3 gene: cloning of a novel Id3 isoform expressed during vascular lesion formation in rat and human atherosclerosis. *Arterioscler Thromb Vasc Biol*. 2001;21:752–758.
54. Habashi JP, Judge DP, Holm TM, Cohn RD, Loeys BL, Cooper TK, Myers L, Klein EC, Liu G, Calvi C, Podowski M, Neptune ER, Halushka MK, Bedja D, Gabrielson K, Rifkin DB, Carta L, Ramirez F, Huso DL, Dietz HC. Losartan, an AT₁ antagonist, prevents aortic aneurysm in a mouse model of Marfan syndrome. *Science*. 2006;312:117–121.
55. Thomas JA, Deaton RA, Hastings NE, Shang Y, Moehle CW, Eriksson U, Topouzis S, Wamhoff BR, Blackman BR, Owens GK. PDGF-DD, a novel mediator of smooth muscle cell phenotypic modulation, is upregulated in endothelial cells exposed to atherosclerosis-prone flow patterns. *Am J Physiol Heart Circ Physiol*. 2009;296:H442–H452.

Novelty and Significance

What Is Known?

- In cultured cells, Ang II predominantly promotes hypertrophy of SMCs, although some studies demonstrate proliferation.
- Ang II induces the generation of ROS.
- Id3 promotes SMC proliferation.

What New Information Does This Article Contribute?

- Ang II induced both aortic SMC hypertrophy and hyperplasia in a region-specific manner, in vivo, independent of blood pressure.
- Ang II-mediated hypertrophy and hyperplasia were dependent on AT_{1a} receptors and ROS.
- Ang II-induced hyperplasia in the ascending aorta was inhibited by Id3 deficiency.

Angiotensin II (Ang II) infusions induce several distinct vascular pathologies that are region-specific in the aorta. In vitro

experiments have implicated smooth muscle cells (SMCs) as having a role in these pathologies. The objective of this study was to define region-specific effects of Ang II infusion in the aortic media and define mechanisms for the differences in vivo. Infusions of Ang II into normolipidemic mice for 28 days promoted equivalent medial thickening throughout the aorta because of stimulation of angiotensin II type 1a (AT_{1a}) receptors but was independent of blood pressure changes. This thickening was attributable to increased SMC size; except in the ascending aortic region where there was a profound increase in SMC-associated nuclei. The medial changes, in all regions, were ablated by the inability to form reactive oxygen species (ROS) by the NADPH oxidase system, as demonstrated in p47^{phox}-deficient mice. However, the Ang II-induced increases in numbers of ascending aortic nuclei was ablated by the deficiency of inhibitor of differentiation 3 (Id3). This is the first study to demonstrate that Ang II induces SMC hypertrophy with Id3-dependent, region-specific proliferation in the aortic arch. These studies provide a basis for defining the role of Id3 in the Ang II-induced pathology of the ascending aorta.

SUPPLEMENT MATERIAL

Angiotensin II Induces a Region-Specific Hyperplasia of the Ascending Aorta Through Regulation of Inhibitor of Differentiation 3

A. Phillip Owens III^{1,2}, Venkateswaran Subramanian², Jessica J. Moorleghen²,
Zhenheng Guo², Coleen A. McNamara⁴, Lisa A Cassis^{1,3}, and Alan Daugherty^{1,2,3}

Graduate Center for Toxicology¹
Cardiovascular Research Center²
Graduate Center for Nutritional Sciences³
University of Kentucky
Lexington, KY 40536

Department of Internal Medicine, Cardiovascular Division, and
Cardiovascular Research Center⁴
University of Virginia
Charlottesville, VA 22908

Condensed title: Angiotensin II, Aortic Hyperplasia, and Id3

Address for Correspondence: Alan Daugherty
Cardiovascular Research Center
Wethington Building, room 521
University of Kentucky
Lexington, KY 40536-0200
Telephone: (859) 323-4933 x 81389
Fax: (859) 257-3646
E-mail: Alan.Daugherty@uky.edu

SUPPLEMENT MATERIALS AND METHODS

Mice:

AT1a receptor deficient mice (N=10; B6.129P2-Agtr1a^{tm1Unc}; stock no. 002682), C57BL/6 (stock no. 000664), and p47phox mutant mice (B6(Cg)-Ncf1^{m1J}/J, stock no. 004742; backcrossed N ≥ 10 C57BL/6; C57^{p47/p47}) were purchased from the Jackson Laboratory. Littermate controls were utilized for all experiments. Id3^{-/-} mice were a generous gift from Dr. Yuan Zhang (Duke University), and were N ≥ 10 for the C57BL/6 background. Mice were housed in a pathogen-free environment and fed a normal diet (Harlan Teklad catalog No. 2918) and water ad libitum. All studies were performed using male mice. Genotyping for AT1a receptor^{-/-} mice,³ C57^{p47/p47},¹⁰ and Id3^{-/-}¹⁶ mice was performed as described previously.^{1,2,3} All procedures were approved by the University of Kentucky IACUC.

Alzet Pump Implantation:

At 8 to 10 weeks of age, C57BL/6, AT1a receptor^{-/-}, C57^{p47/p47}, and Id3^{-/-} male mice were implanted with Alzet mini-osmotic pumps (Model 2004, Durect Corp), subcutaneously in the right flank and infused with either sterile saline or AngII (Sigma cat# A9525; 1,000 ng/kg/min) for 28 days (n = 5-10), as described previously.¹ In addition, norepinephrine (L-(-)-norepinephrine bitartrate salt (NE), Sigma cat# A9512; 5.6 mg/kg/day) was infused into C57BL/6, AT1a receptor^{-/-}, and C57^{p47/p47} mice (n=5 each group).²⁰ NE was dissolved in L-ascorbic acid/saline (Fisher cat# A61; 0.2% wt/vol) as described previously.¹⁸ N_ω Nitro-L-arginine methyl ester hydrochloride (Sigma cat# N5751) was introduced via the drinking water at a concentration of 1.5 mg/ml (~100 mg/kg/day, changed daily).¹¹

Systolic Blood Pressure Measurement:

SBP was measured noninvasively on conscious mice using the Visitech tail cuff system (BP-2000 Visitech Systems). Mice were habituated 1.5 weeks prior to pump implantations and SBP was measured 5-6 times a week, at the same time of day, throughout the entire infusion period, as described previously.²

Tissue Preparation:

Mice were anesthetized with ketamine/xylazine, blood was collected with EDTA (0.2% wt/vol) from the right ventricle, and exsanguination was performed via an incision in the right atria. Aortas were perfused via the left ventricle with phosphate-buffered saline and then perfusion fixed with paraformaldehyde (4% wt/vol) under physiological pressure for 30-45 minutes. Organs were removed and aortas were filled, via the left cardiac ventricle, with low melting point agarose (Promega cat# V2111; 3% wt/wt) and colored with a green tissue dye (Polysciences, Inc. cat# 24110), as described previously.¹⁹ Ascending aortic sections were located 1 to 3 mm distal to termination of valve leaflet stubs. Thoracic sections were located between 5 mm and 7 mm posterior of the left subclavian artery. Suprarenal abdominal aortic sections were flush with the superior mesenteric artery and 2 mm anterior. Infrarenal abdominal aortic sections were 2 mm cut from the left renal branch to the posterior. These aortic sections are schematically represented in Online Figure I. Aortic sections were placed in OCT (Tissue-Tek cat# 4583) and cut serially in 10 μm increments (posterior to anterior) with 9 sections per slide and a total of 8 slides. With the exception of ascending arch aortas (no branch points), all branch points and aortic vessels were discarded, leading to the final coverage of approximately 900 to 1500 μm of aorta per cross-sectional slide.

Morphometric Analyses:

Sections were stained with hematoxylin-eosin, mounted with glycerol/gelatin (Sigma), and captured on a Nikon Optiphot-2 with a Nikon DXM camera. The inner elastic lamina was traced and subtracted from the outer elastic lamina to measure medial areas. Medial thickness was calculated from means of 4 orthogonal measures of the distances between the internal and external elastic lamina. Mean medial areas and thicknesses were measured from 5 to 15 sections per mouse. Measurements were performed using Image Pro-Plus 5.0 software (Media Cybernetics).

Nuclei Counting:

Frozen sections were fixed in paraformaldehyde (4% wt/vol). Propidium iodide staining (Molecular Probes, P-3566, 1 µg/ml) was performed, subsequently to RNA digestion for 15 min at 37°C. The nuclei counts were quantitated on 2 aortic segments of equivalent length (0.25 mm) per serial section (minimum of 6 sections per slide).

Aortic Immunostaining and Histology:

Histological analysis was performed on paraformaldehyde fixed frozen sections using Movat's pentachrome (PolyScientific, cat# K042). Immunostaining was performed on frozen serial sections as described previously.¹⁴ An α-actin SMC antibody (5 µg/ml; Abcam, cat# ab5694) was incubated for 30 minutes at 37°C.¹⁵ Subsequent application of a goat antirabbit biotinylated antibody (1:500; Vector) was incubated for 30 minutes at 37°C. Positive reactive areas were visualized via application of an ABC kit (10 minutes 37°C) and subsequent detection with AEC chromogen (2 applications of 10 minutes 37°C; Vector). Several controls were used, including: no primary antibody, no primary and secondary antibodies, and non-immune IgG (Online Figure II).¹⁵ Images were captured with a 20x objective lens using a Nikon Eclipse E600 scope and a Nikon DXM1200F digital camera.

SMC Isolation:

Aortas from 8-10 week old male C57BL/6J mice (Jackson Laboratory) were isolated and dissected free of adventitia in serum-free Dulbecco's Modified Eagle's Medium (DMEM). Aortas were divided into four sections: ascending aorta (above the heart to left subclavian artery), thoracic aorta (left subclavian artery to last intercostal artery), suprarenal aorta (last intercostal artery to right renal artery), and infrarenal aorta (left renal artery to iliac bifurcation). SMCs were isolated via chemical digestion using type III porcine pancreatic elastase (250 µg/ml, Sigma) and type I collagenase (1 µg/ml, Worthington), as described previously.¹⁷ SMCs were maintained in DMEM with fetal bovine serum (20% vol/vol; FBS, Equitech, Inc.) and penicillin and streptomycin (1% wt/vol, Gibco) in a 37°C incubator with 5% CO₂. SMC phenotype was determined via visualization with Cy3 labeled α-actin clone 1A4 (Sigma).

Cellular Immunofluorescence and Confocal Microscopy:

SMCs were isolated as described above, and grown on glass Lab-Tek chamber slides (Nunc) (n=6 separate samples each section). At 70% confluency, cells were washed, and subsequently incubated with serum-free media. After 72 hours, wells were rinsed with PBS, and incubated with either saline or AngII (1 µM) for 1, 2, 12, and 24 hours. Slides were then rinsed with PBS and fixed with paraformaldehyde (4% wt/vol) for 10 minutes. Cells were permeabilized with Triton X-100 (0.5% vol/vol) in PBS for 10 minutes at 37°C. Non-specific binding was blocked via incubation with normal goat serum (15 µg/ml) and BSA (1% wt/vol) for 30 minutes at 37°C. A rabbit monoclonal Id3 primary antibody (5 µg/ml; Cal Bioreagents, clone 6-1) was incubated overnight in a humidity chamber at 4°C. After washing 3 times in PBS,

secondary goat antirabbit labeled Cy2 (1:250 dilution, Jackson Immuno) and Cy3-labeled α -SMC actin (1:100 dilution, clone 1A4, Sigma) were added for 30 minutes at 37°C. Chambers were subsequently washed 3 times with PBS and then incubated with Hoechst 33342 (1 μ g/ml; Invitrogen) for 5 minutes. Chambers were removed, slides were mounted with aqueous mounting media (Biomedica Corp), and coverslips were fixed in place using clear nail polish. Controls were included using no addition of primary antibody, no addition of either primary or secondary antibodies, and rabbit IgG control (5 μ g/ml). Slides were visualized and captured using an Olympus BX61WI confocal microscope and FluoView software.

SMC Proliferation Analyses:

SMCs were isolated, as described above, counted using a hemacytometer, and seeded onto 35 x 10 mm culture wells at 10,000 cells/well. Separate primary harvests from 5 different groups of 8-10 week old male C57BL/6 mice (Jackson Laboratory) were performed. Cells were immediately serum-starved for 24 hours and then incubated with saline, AngII (1 μ M), or PDGF-BB (25 ng/ml; Sigma) for 24, 48, or 72 hours. Saline, AngII, or PDGF-BB were incubated with cells in the presence of FBS (2.5% vol/vol; which did not induce changes in cell numbers). Wells were washed 3 times using PBS and cells removed using trypsin-EDTA (0.25% wt/vol; Gibco), quenched with FBS, and subsequently counted using a hemacytometer. Cell numbers were also verified on a Hemavet 950 (Drew Scientific) cell counter.

Dichlorodihydrofluorescein diacetate (DCF-DA) Analyses:

SMCs were isolated, as described above, plated on glass Lab-Tek chamber slides, and grown to ~70-80% confluency in DMEM with FBS (20% vol/vol; n=5 separate samples each section). Cells were then serum-starved for 24 hours in DMEM, and subsequently incubated with AngII (1 μ M), AngII (1 μ M) + losartan (1 μ M), saline, H₂O₂ control (1 μ M), or saline no DCF-DA blank control. DCF-DA (Invitrogen) reagent was incubated with cells after 24 hours of incubation. Chamber slides were subsequently visualized using a Nikon Eclipse E600 scope with excitation sources and filters appropriate for fluorescein (FITC) detection.

Amplex Red Analyses:

SMCs were isolated, as described above, plated on 6-well culture plates, and grown to ~70-80% confluency in DMEM with FBS (20% vol/vol; n=4 separate samples each section). Cells were serum-starved for 24 hours and incubated with saline, AngII (1 μ M), or AngII (1 μ M) + PEG-catalase (100 U/ml, Sigma) for an additional 24 hours. Amplex red assay (Invitrogen) was performed using modifications described previously in the protocol.²¹ Fluorescence intensity was determined using a microplate reader (Molecular Devices, SpectroMax M2) in the excitation range of 530-560 nm and emission detection at 590 nm. SMCs were incubated with standard lysis buffer, protein was extracted, and examined using a Bradford Assay (Bio-Rad). Fluorescent readings were subsequently normalized to cellular protein content.

Detection of Extracellular Superoxide using Cytochrome c Reduction Assay

Two arterial rings (2 mm) were each isolated from the arch, thorax, suprarenal, and infrarenal regions of aortas dissected from C57BL/6 mice (n = 32 mice; n = 4 separate samples). Briefly, aortas were removed, 2 aortic pieces per region were placed into DMEM containing FBS (5%) and incubated with either with saline or AngII (1 μ M) for 24 hours. Aortic segments were washed in sterile PBS and placed into modified Krebs/HEPES buffer additionally containing deferoxamine mesylate (100 μ M, Sigma

D9533) and PEG-catalase (100 U/ml, Sigma). Cytochrome c (50 μ M, Sigma C4186) was added and the samples were incubated at 37° C for 1 hour with or without PEG-SOD (200 U/ml, Sigma S9549). Cytochrome c reduction was calculated via absorbances on a microplate reader (Molecular Devices, SpectroMax M2) at 540, 550, and 560 utilizing the following equation: $550 - ((540+560)/2)$. Formation of superoxide was calculated using the following equation $((\Delta OD \text{ without SOD} - \Delta OD \text{ with SOD}) / 21.1 \text{ mM}^{-1} \text{ cm}^{-1})$. Superoxide production was normalized to tissue protein concentration using a Bradford Assay (Bio-Rad).^{8,12,13}

Detection of Intracellular Superoxide using High Performance Liquid Chromatography (HPLC)

Alzet pumps containing saline or AngII (1000 ng/kg/min) were implanted into 8-10 week old male C57BL/6J mice (Jackson Laboratory) for 14 days (n = 5 per group). Mice were then euthanized, aortas extracted, placed in ice-cold modified Krebs/HEPES buffer, and quickly cleaned free of adventitia. Arterial rings (2 mm) were obtained from each aortic region, as described above, and incubated with dihydroethidium (DHE, 50 μ M, Molecular Probes) in modified Krebs/HEPES buffer for 30 min at 37°C. Tissues were then homogenized in methanol (300 μ l) using a glass mortar and pestle. Aliquots were used for protein determination (Nanodrop 8000 spectrophotometer; Nanodrop Products, Wilmington, DE) and HPLC analysis. A Beckman HPLC System Gold model with a C-18 reverse phase column (Nucleosil 250-4.5 mm), equipped with both UV and fluorescence detectors was used to separate 2-hydroxyethidium (2-OH-E⁺) and ethidium from DHE. Fluorescence detection at 580 nm (emission) and 480 nm (excitation) was used to monitor oxyethidium production. UV absorption at 355 nm was used for detection of DHE. The mobile phase was composed of a gradient containing 100% acetonitrile and 0.1% trifluoroacetic acid. DHE, 2-OH-E⁺, and ethidium were resolved using a linear gradient of acetonitrile from 32 to 47% over 25 minutes at a flow rate of 0.5 ml/min. 2-OH-E⁺ was calculated from peak area and subsequently compared to a DHE control (50 μ M) peak and normalized to protein (mg).

Apoptosis Analysis via Tdt-mediated dUTP nick end labeling (TUNEL):

SMCs were isolated, as described above, plated on glass Lab-Tek chamber slides, and grown to ~80% confluency in DMEM with FBS (20% vol/vol; n=5 separate samples each section). Cells were serum-starved for 24 hours and subsequently incubated with saline, AngII (1 μ M), or Staurosporine (1 μ M, Sigma) for 24 hours. Apoptotic cells were detected using the in situ cell death TUNEL detection assay according to manufacturer's instructions (Roche Applied Sciences, Cat# 12156792910). Nuclei were stained with Hoechst 33342 (1 μ g/ml; Invitrogen) for 5 minutes, and the slides were subsequently examined via fluorescent microscopy. The percentage of TUNEL-positive cells (relative to total SMCs) were determined by counting ~200 to 300 cells in 10 randomly chosen fields per well for each aortic segment and each experiment.

Renin Analyses:

Blood was collected in syringes filled with EDTA (0.2 M) and centrifuged at 2,000 rpm for 20 minutes for plasma collection. Renin concentrations in plasma (8 μ l) were measured by incubation with an excess of angiotensinogen (0.4 μ M; Sigma) in the presence of EDTA (0.02 M) for 30 min at 37°C. AngI generated was quantified by RIA using a commercially available kit (Diagnostic Systems Laboratories).⁹

Cell Culture and Western Blot Analyses:

SMCs were isolated, as described above, and plated on 6-well culture plates in DMEM with FBS (20% vol/vol). Separate primary harvests from 3 different groups of 8-10 week old male C57BL/6 mice (Jackson Laboratory) were performed. At ~70-80% confluency, wells were washed 3 times with PBS and serum-starved for 72 hours, as described previously.⁷ Cells were then incubated with either saline or AngII (1 μ M) for 1, 2, 12, or 24 hours and total cell lysates were extracted using 1x cell lysis buffer (cat: 9803; Cell Signaling) with addition of protease inhibitor cocktails. Protein content was measured using a Bradford Assay (Bio-Rad) and subsequently equal amounts of protein (20 μ g) were resolved using SDS-PAGE (12.5% wt/vol), and transferred via electrophoresis (50 V for 90 minutes) to PVDF membranes (Millipore). Membranes were blocked at room temperature with nonfat milk (5% wt/vol) in Tris-buffered saline, containing tween 20 (0.5% vol/vol; TBS-T). Membranes were cut at the 25 kD molecular weight marker and the lower section was incubated with an antibody against Id3 (0.5 μ g/ml, clone 6-1, Cal Bioreagents). The upper section was incubated with a β -actin antibody (1:1000, Sigma) overnight at 4°C. Horseradish peroxidase-conjugated secondary antibodies were incubated for 1 hour and immune complexes were visualized by a Supersignal West Pico Chemiluminescence Kit (Pierce) and quantified using a Kodak Imager.

Real Time Polymerase Chain Reaction:

Ascending (aortic sinus to left subclavian), thoracic (left subclavian to last intercostal), suprarenal (last intercostal to right renal), and infrarenal (left renal to iliac bifurcation) sections of aortas were harvested from thirty 8 week old male C57BL/6 and placed in RNA Later (Ambion, cat# 7024), and adventitia was removed. Aortas were combined, in groups of 5, for a total of 6 independent samples for each section. Aortas were ground with a glass mortar and pestle in the presence of lysis buffer (Rneasy Fibrous Minikit Isolation System, Qiagen, cat# 74704). All samples were incubated with Turbo DNA-free (Ambion, cat# AM1907) to remove all DNA contamination. RNA concentrations were quantified using a UV spectrophotometer (Beckman DU530). Reverse transcription of RNA was performed with i-script (Bio-Rad, cat# 170-8891) with a concentration of 100 ng total RNA using an i-cycler (Bio-Rad). Real-time analysis of cDNA amplifications were performed using a Bio-Rad i-cycler with Id3 Taqman probes (Applied Biosystems, catalog# Mm00492575-m1) and IQ supermix (Bio-Rad, cat# 170-8860). These results were compared to an 18s rRNA endogenous control (Applied Biosystems, cat# 4352930E). Results were extrapolated using the standard curve method with kidney serving as the Id3 standard. Negative controls consisted of no RT controls and Id3^{-/-} tissue cDNA, which was not detectable with these primers. Another separate run was performed and stopped in the middle of the sigmoidal real-time curve. These samples were run on agarose gels (3% wt/vol) diluted with a 6x blue-green running dye and molecular weight was analyzed with a PGEM DNA marker (Promega).

Statistics:

All statistical analyses were performed using either SigmaStat (SPSS Inc.) or version 8.2 of SAS (SAS Institute). All measurements are represented as means \pm SEM. One Way ANOVA was performed on measurements, where indicated, with a Holm-Sidak post hoc test. For two group comparison of parametric data, a Student's t-test was performed. Repeated measures data were analyzed with SAS fitting a linear mixed model expressing the temporal trend in systolic blood pressure as a quadratic polynomial in time for each treatment. A Bonferroni-adjusted pairwise comparison was

performed within similar genotypes among treatments.

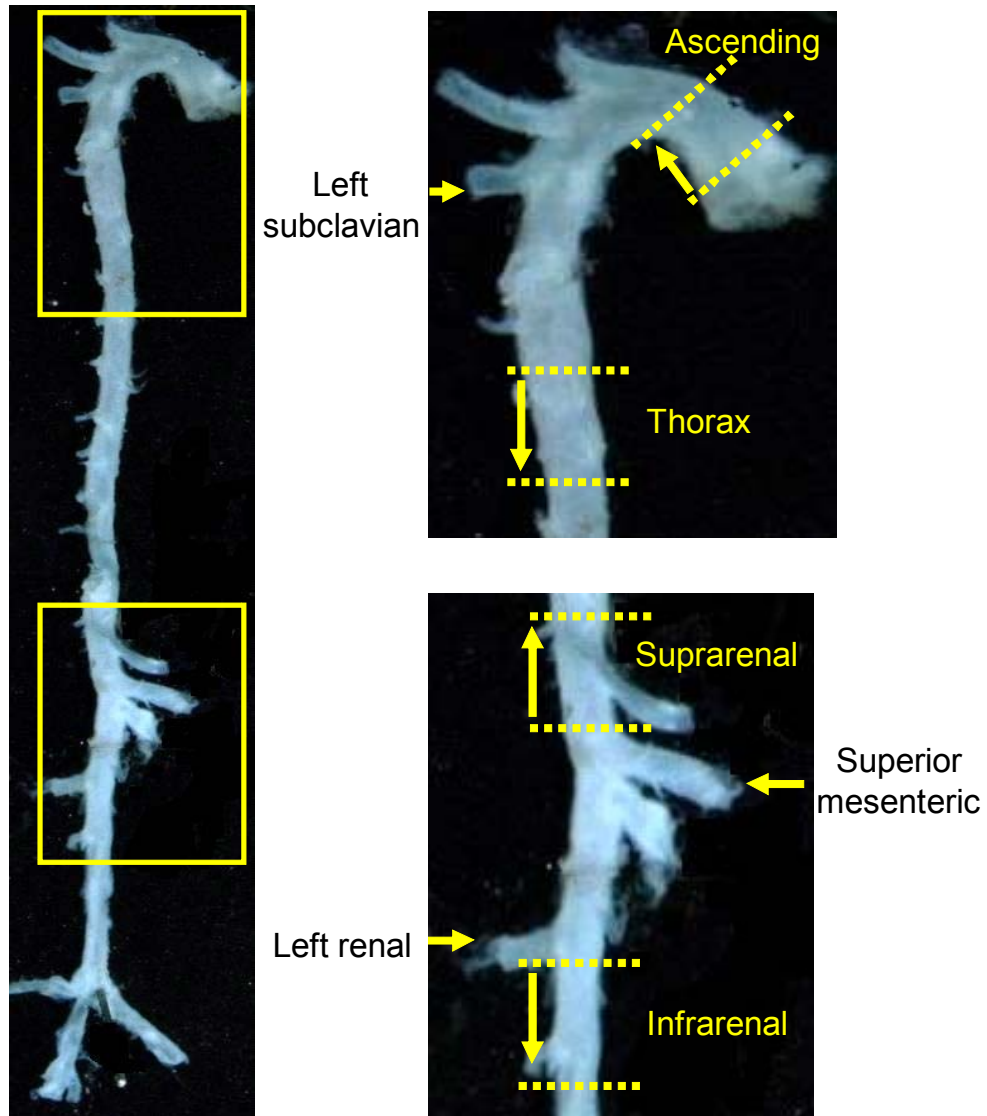
REFERENCES

1. Daugherty A, Manning MW, Cassis LA. Angiotensin II promotes atherosclerotic lesions and aneurysms in apolipoprotein E-deficient mice. *J Clin Invest.* 2000;105:1605-1612.
2. Daugherty A, Manning MW, Cassis LA. Antagonism of AT2 receptors augments angiotensin II-induced abdominal aortic aneurysms and atherosclerosis. *Br J Pharmacol.* 2001;134:865-870.
3. Daugherty A, Rateri DL, Lu H, Inagami T, Cassis LA. Hypercholesterolemia stimulates angiotensin peptide synthesis and contributes to atherosclerosis through the AT1A receptor. *Circulation.* 2004;110:3849-3857.
4. Dikalov S, Griendling KK, Harrison DG. Measurement of reactive oxygen species in cardiovascular studies. *Hypertension.* 2007;49:717-27.
5. Dikalova A, Clempus R, Lassegue B, Cheng G, McCoy J, Dikalov S, San Martin A, Lyle A, Weber DS, Weiss D, Taylor WR, Schmidt HH, Owens GK, Lambeth JD, Griendling KK. Nox1 overexpression potentiates angiotensin II-induced hypertension and vascular smooth muscle hypertrophy in transgenic mice. *Circulation.* 2005;112:2668-2676.
6. Fink B, Laude K, McCann L, Doughan A, Harrison DG, Dikalov S. Detection of intracellular superoxide formation in endothelial cells and intact tissues using dihydroethidium and an HPLC-based assay. *Am J Physiol Cell Physiol.* 2004;287:C895-902.
7. Forrest ST, Taylor AM, Sarembock IJ, Perlegas D, McNamara CA. Phosphorylation regulates Id3 function in vascular smooth muscle cells. *Circ Res.* 2004;95:557-559.
8. Gongora MC, Qin Z, Laude K, Kim HW, McCann L, Folz JR, Dikalov S, Fukai T, Harrison DG. Role of extracellular superoxide dismutase in hypertension. *Hypertension.* 2006;48:473-81.
9. Henriques TA, Huang J, D'Souza SS, Daugherty A, Cassis LA. Orchidectomy, but not ovariectomy, regulates angiotensin II-induced vascular diseases in apolipoprotein E-deficient mice. *Endocrinology.* 2004;145:3866-3872.
10. Huang CK, Zhan L, Hannigan MO, Ai Y, Leto TL. P47(phox)-deficient NADPH oxidase defect in neutrophils of diabetic mouse strains, C57BL/6J-m db/db and db/+. *J Leukoc Biol.* 2000;67:210-5.
11. Kojda G, Laursen JB, Ramasamy S, Kent JD, Kurz S, Burchfield J, Shesely EG, Harrison DG. Protein expression, vascular reactivity and soluble guanylate cyclase activity in mice lacking the endothelial cell nitric oxide synthase: contributions of NOS isoforms to blood pressure and heart rate control. *Cardiovasc Res.* 1999;42:206-13.
12. Kolbeck RC, She ZW, Callahan LA, Nosek TM. Increased superoxide production during fatigue in the perfused rat diaphragm. *Am J Respir Crit Care Med.* 1997;156:140-5.
13. Landmesser U, Dikalov S, Price SR, McCann L, Fukai T, Holland SM, Mitch WE, Harrison DG. Oxidation of tetrahydrobiopterin leads to uncoupling of endothelial cell nitric oxide synthase in hypertension. *J Clin Invest.* 2003;111:1201-9.
14. Lu H, Rateri DL, Daugherty A. Immunostaining in mouse atherosclerosis. *Methods Mol Biol.* 2007;139:77-94.
15. Lu H, Rateri DL, Feldman DL, Charnigo Jr. RJ, Fukamizu A, Ishida J, Oesterling

- EG, Cassis LA, Daugherty A. Renin inhibition reduces hypercholesterolemia-induced atherosclerosis in mice. *J Clin Invest*. 2008;118:in press.
16. Lyden D, Young AZ, Zagzag D, Yan W, Gerald W, O'Reilly R, Bader BL, Hynes RO, Zhuang Y, Manova K, Benezra R. Id1 and Id3 are required for neurogenesis, angiogenesis and vascularization of tumour xenografts. *Nature*. 1999;401:670-7.
 17. Ray JL, Leach R, Herbert JM, Benson M. Isolation of vascular smooth muscle cells from a single murine aorta. *Methods Cell Sci*. 2001;23:185-8.
 18. Vecchione C, Fratta L, Rizzoni D, Notte A, Poulet R, Porteri E, Frati G, Guelfi D, Trimarco V, Mulvany MJ, Agabiti-Rosei E, Trimarco B, Cotecchia S, Lembo G. Cardiovascular influences of alpha1b-adrenergic receptor defect in mice. *Circulation*. 2002;105:1700-1707.
 19. Wang YX, Martin-McNulty B, Freay AD, Sukovich DA, Halks-Miller M, Li WW, Vergona R, Sullivan ME, Morser J, Dole WP, Deng GG. Angiotensin II increases urokinase-type plasminogen activator expression and induces aneurysm in the abdominal aorta of apolipoprotein E-deficient mice. *Am J Pathol*. 2001;159:1455-1464.
 20. Weiss D, Kools JJ, Taylor WR. Angiotensin II-induced hypertension accelerates the development of atherosclerosis in apoE-deficient mice. *Circulation*. 2001;103:448-454.
 21. Zhou M, Diwu Z, Panchuk-Voloshina N, Haugland RP. A stable nonfluorescent derivative of resorufin for the fluorometric determination of trace hydrogen peroxide: applications in detecting the activity of phagocyte NADPH oxidase and other oxidases. *Anal Biochem*. 1997;253:162-8.

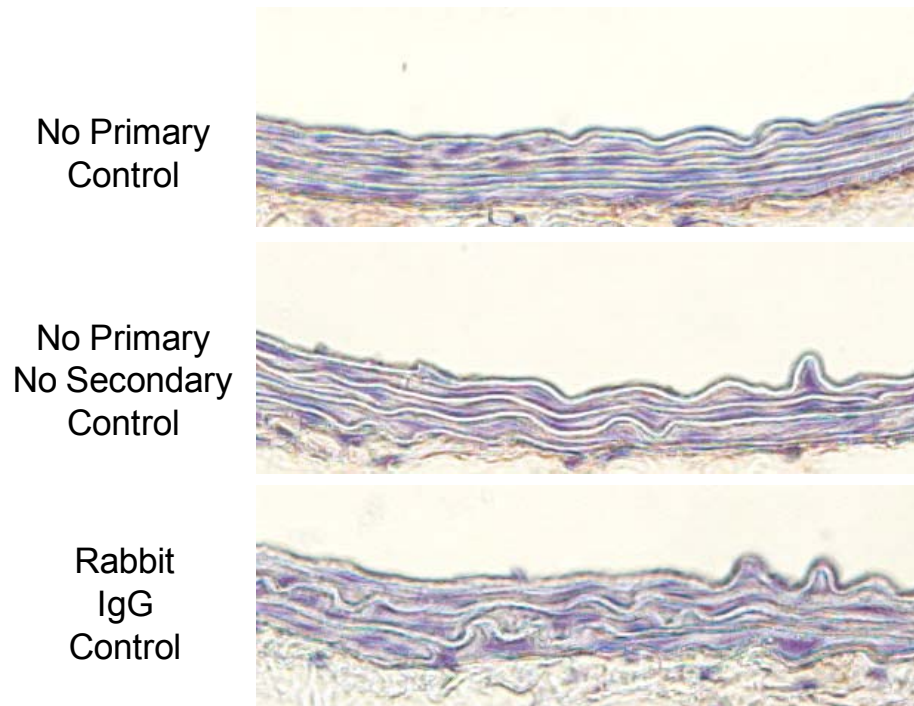
SUPPLEMENT FIGURES

Online Figure I



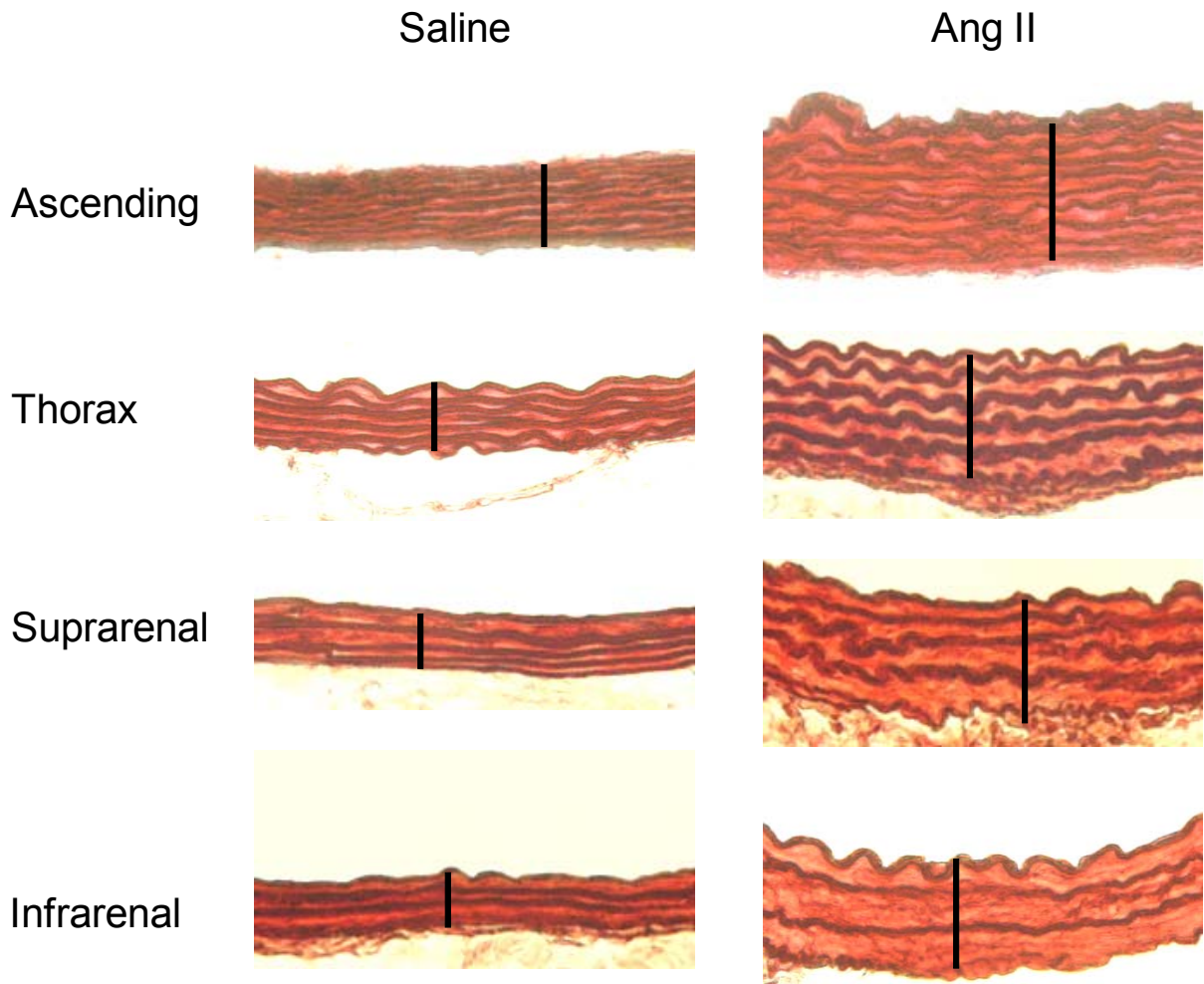
Online Figure I. Schematic diagram of analyzed regional aortic segments. The left subclavian, superior mesenteric, and left renal arteries represent landmarks for standardization between animals. Dashed yellow lines indicate cuts in the aorta, while arrows represent direction of sectioning from start to finish.

Online Figure II



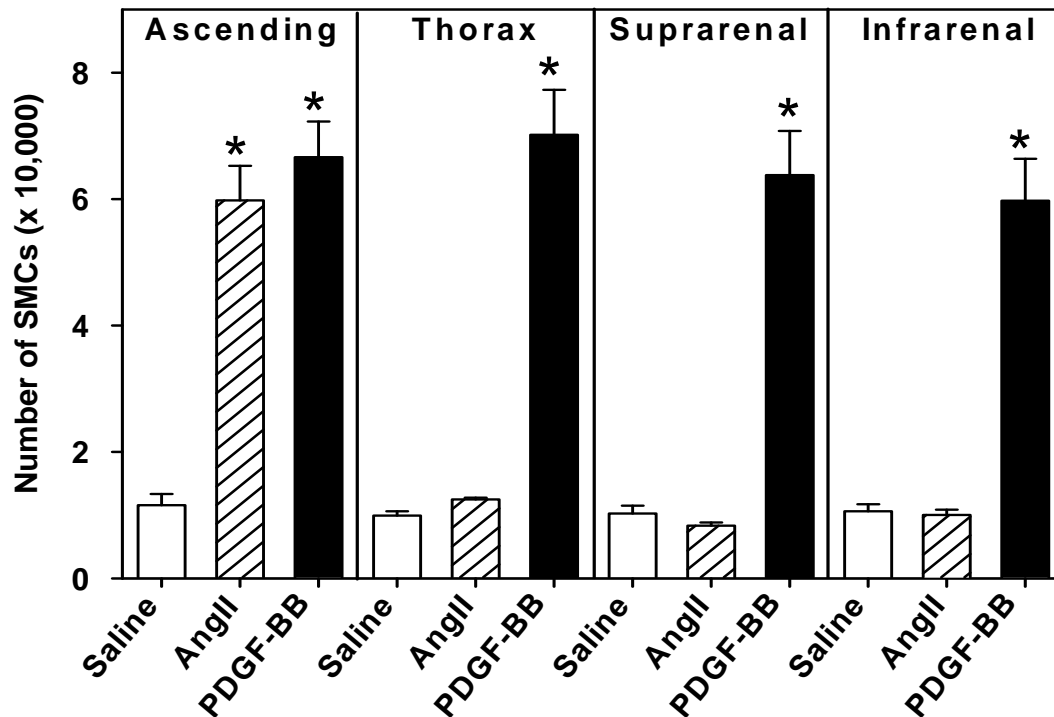
Online Figure II. Controls for the SMC α -actin immunostaining. Tissue sections were incubated under the following conditions: (A) No primary antibody control incubated with secondary antibody (1:500 dilution) only, (B) no primary and no secondary antibody control, and (C) rabbit IgG control (5 μ g/ml).

Online Figure III



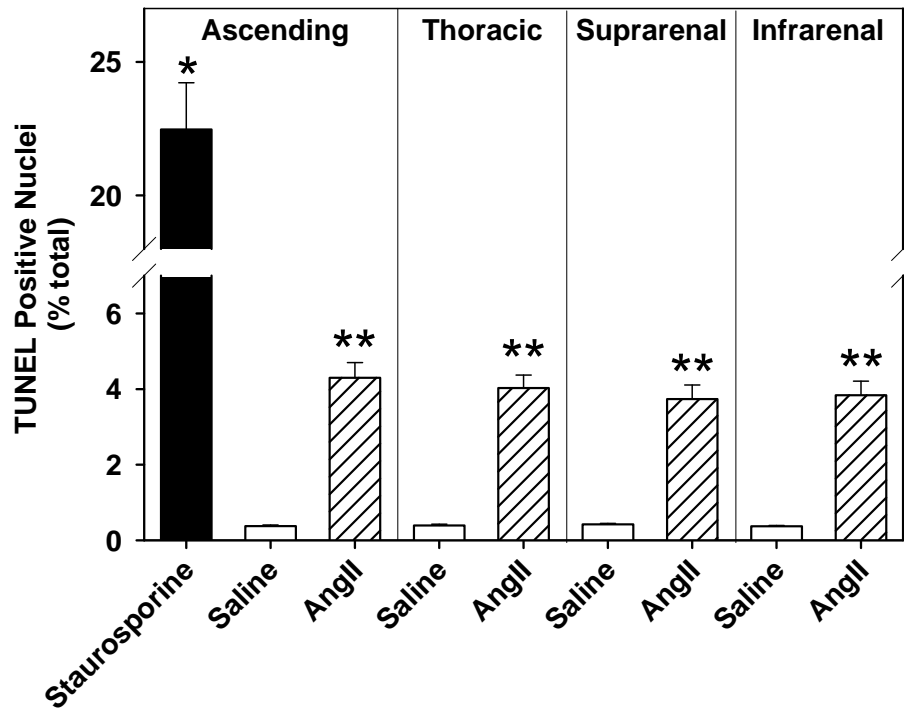
Online Figure III. Movat's pentachrome staining of sections of aortas from mice infused with either saline or AngII. The following denotes specific cellular content and the visual color associated: muscle (red), ground substance (blue/green), elastin fibers (black), and collagen and reticulum fibers (yellow).

Online Figure IV



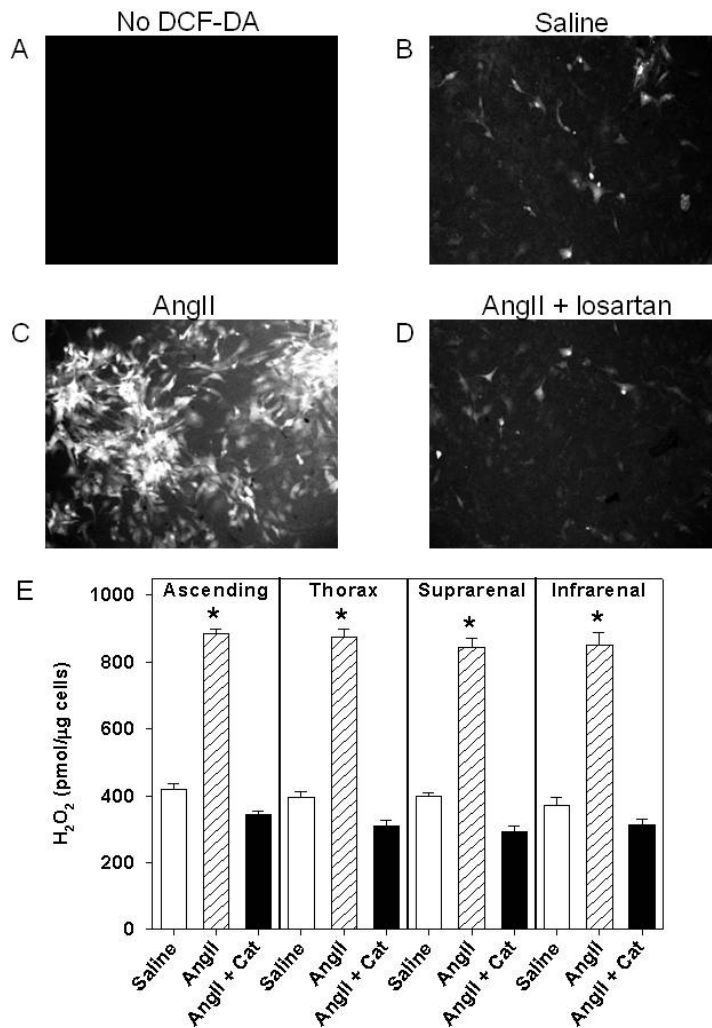
Online Figure IV. AngII induces cellular proliferation in SMCs harvested from ascending aortas. SMCs harvested from specific regions were seeded at day 0 with 10,000 cells/well, serum starved for 24 hours, and subsequently incubated for 72 hours with saline, AngII (1 μ M), or PDGF-BB (25 ng/ml). Histograms are means of 5 individual experiments and bars represent SEM. * Denotes $P < 0.001$ for SMCs from ascending aortas incubated with either AngII or PDGF-BB versus saline, and thoracic, suprarenal, and infrarenal PDGF-BB versus saline and AngII (one-way ANOVA with Holm Sidak post hoc).

Online Figure V



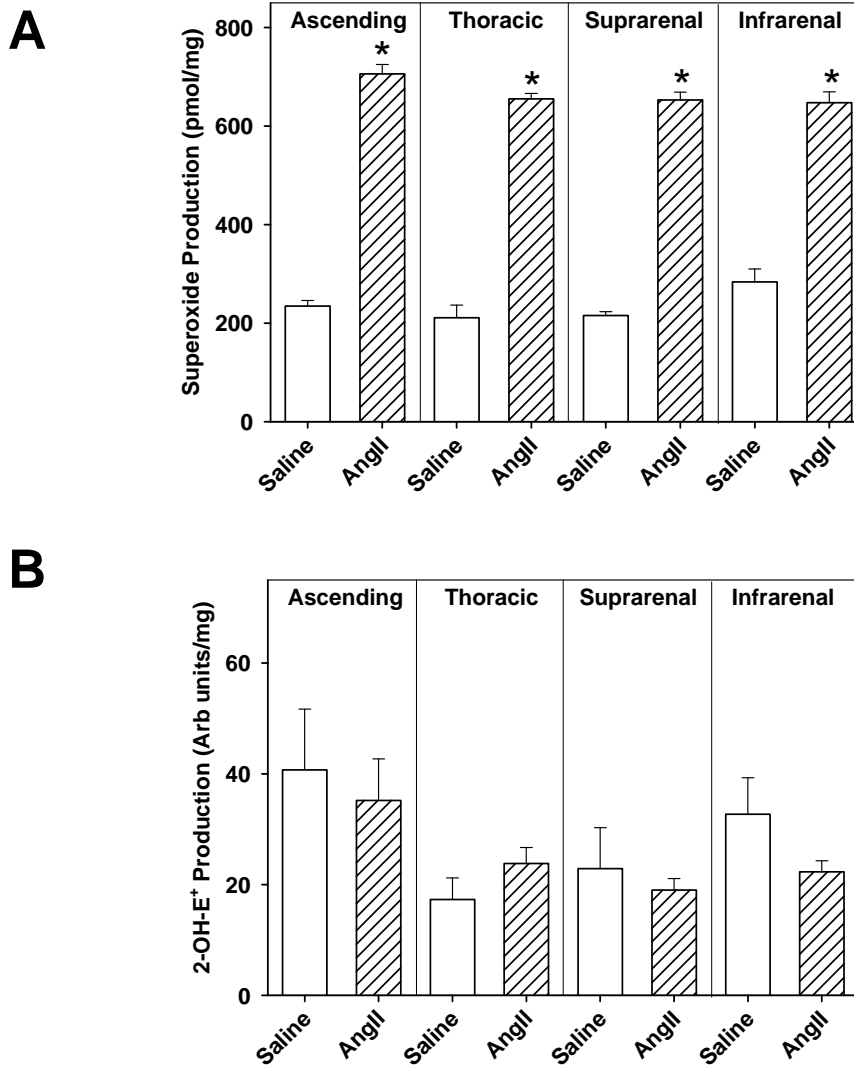
Online Figure V. AngII induces similar rates of apoptosis in SMCs from all aortic regions. SMCs harvested from specific regions were serum starved for 24 hours, and subsequently incubated with saline, AngII (1 μ M), or staurosporine (1 μ M). Apoptosis was detected via TUNEL staining compared to all cells counted (% TUNEL positive). Staurosporine (black histobar) was similar among all groups (arch SMCs represented). Histobars are means of 5 individual experiments and bars represent SEM. * Denotes $P < 0.001$ for SMCs treated with staurosporine compared to all other treatments. ** Denotes $P < 0.01$ for AngII SMCs versus saline SMCs (One Way ANOVA with Holm Sidak post hoc).

Online Figure VI



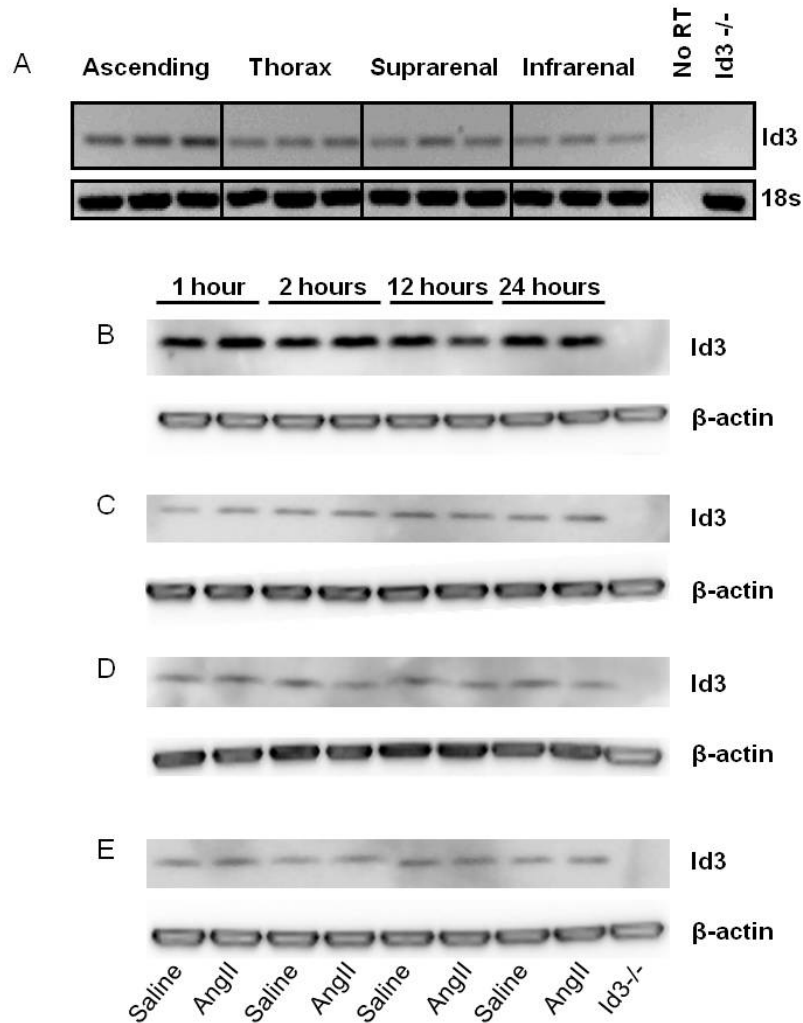
Online Figure VI. AngII induces similar concentrations of ROS *in vitro* in SMCs from all aortic regions. Ascending aortic SMCs were incubated with (A-B) saline, (C) AngII (1 μ M), or (D) AngII (1 μ M) + losartan (1 μ M) for 24 hours and subsequently stained for DCF-DA (except for A). (E) Regional release of H₂O₂ was detected using an Amplex Red assay in SMCs incubated with saline, AngII (1 μ M), or AngII (1 μ M) + PEG-catalase (100 U/ml) for 24 hours. Histograms are means of 4 individual experiments and bars represent SEM. * Denotes $P < 0.001$ in AngII incubated cells versus all other groups (one-way ANOVA with Holm Sidak post hoc).

Online Figure VII



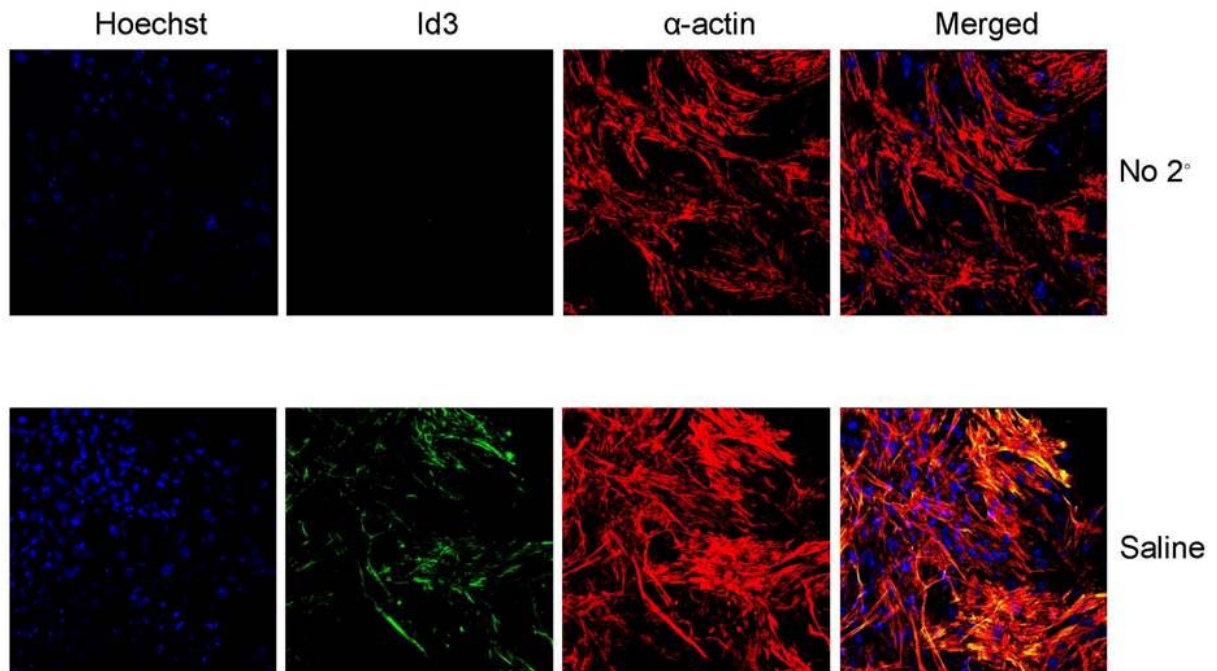
Online Figure VII. Measurement of superoxide in aortic tissues from all regions after *ex vivo* and *in vivo* exposure to AngII. **(A)** Vascular superoxide production was detected in *ex vivo* aortic segments from all aortic segments utilizing the SOD-inhibitable cytochrome c reduction assay. Segments were incubated with saline or AngII (1 μ M) for 24 hours. Histobars represent $n=4$ individual samples and bars represent SEM. * Denotes $P < 0.001$ in AngII incubated segments versus saline, in each region (Mann-Whitney Rank Sum). **(B)** *In vivo* superoxide production was detected in saline and AngII infused mouse aortas (14 days). DHE conversion to 2-OH-E⁺ was measured by HPLC and represented in arbitrary units (Arb units). Histobars represent $n=5$ individual samples and bars represent SEM.

Online Figure VIII



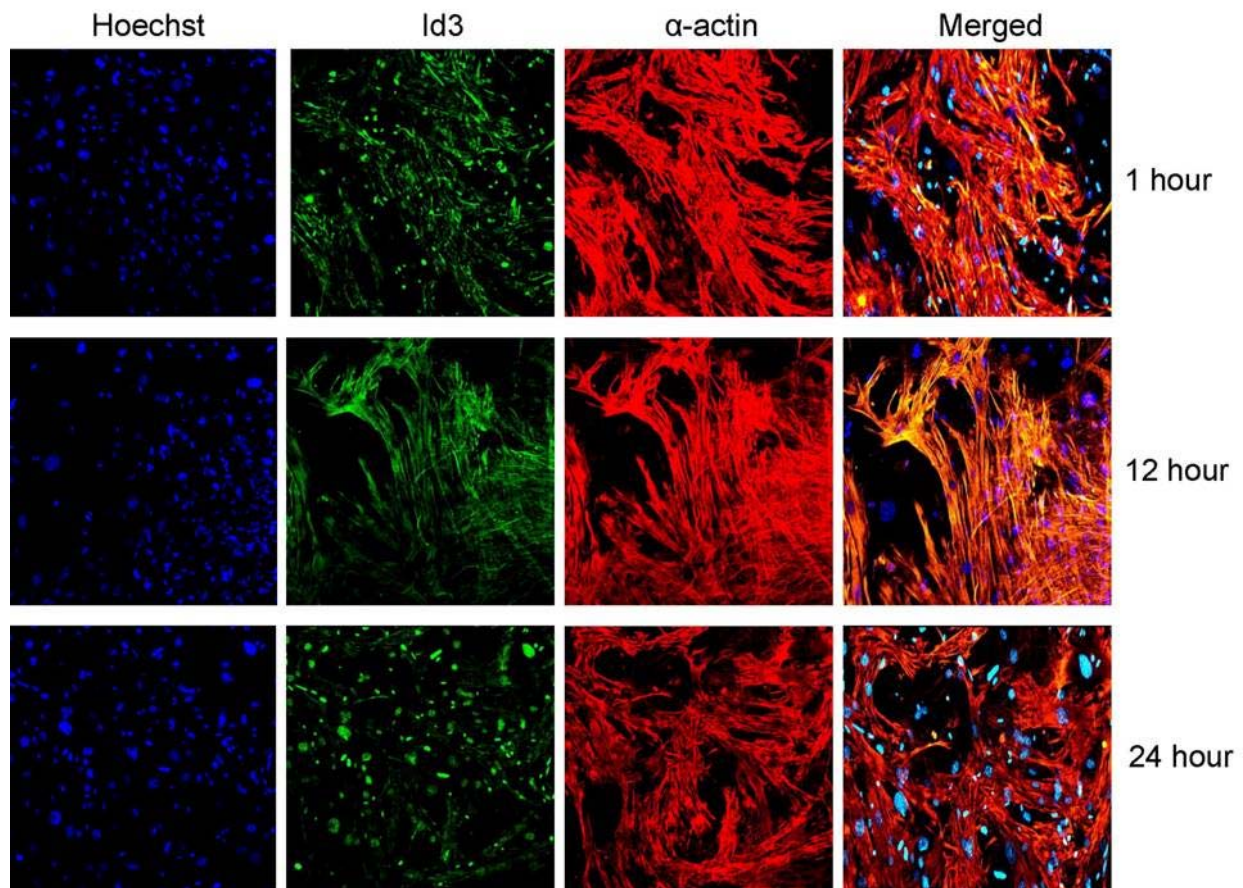
Online Figure VIII. Detection of Id3 mRNA and protein. **(A)** Gel electrophoresis of Id3 mRNA in the 4 aortic regions as indicated. Examples show mRNA resolved on a 3% gel with Id3 (top) and 18s rRNA (bottom) from a qRT-PCR stopped in the middle of the sigmoidal curve. Growth arrested SMCs from **(B)** ascending, **(C)** thoracic, **(D)** suprarenal, and **(E)** infrarenal aortic segments were incubated with either saline or AngII (1 μ M) for 1, 2, 12, or 24 hours. Blots are representative examples from each regional segment, with Id3 analysis (top) and β -actin internal control (bottom). Id3^{-/-} spleen lysate was used for specificity analysis of the Id3 antibody.

Online Figure IX



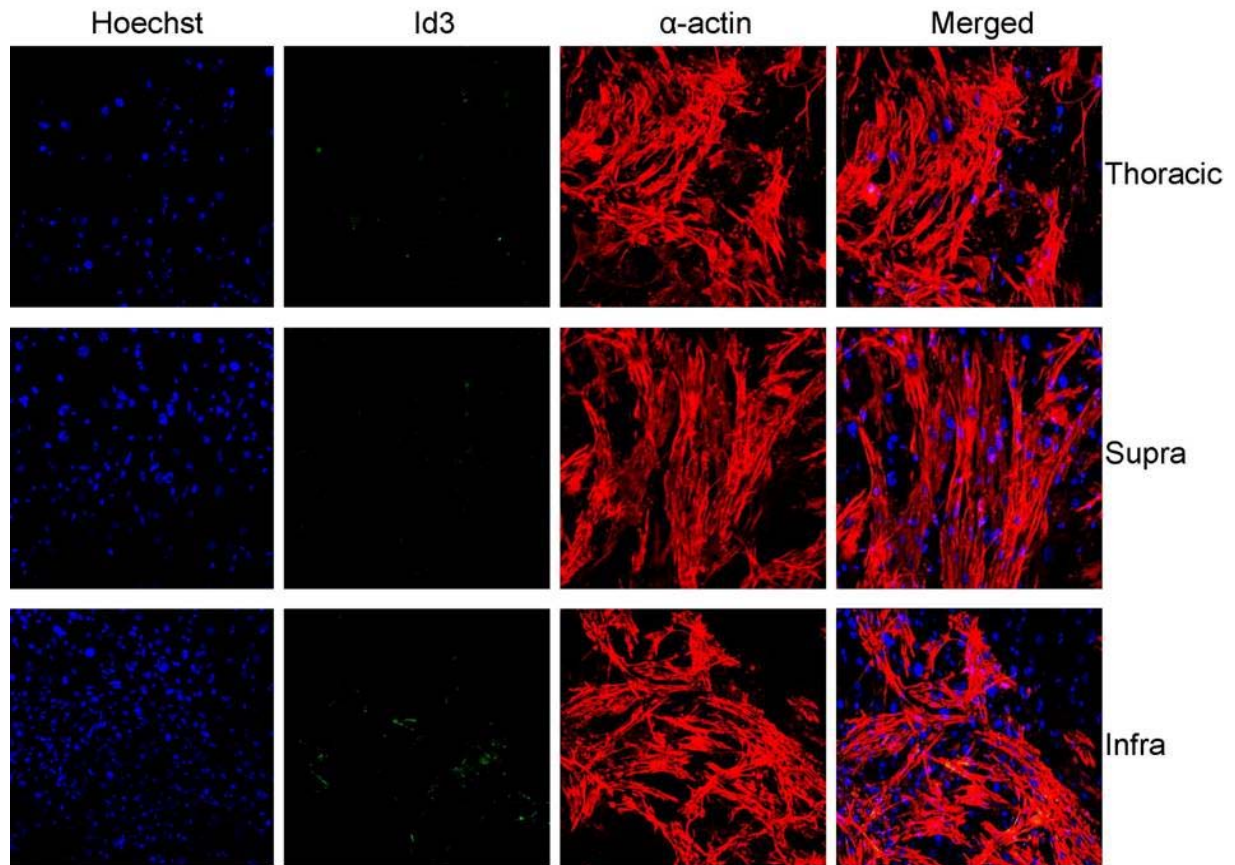
Online Figure IX. Control immunofluorescent staining in SMCs. Ascending aortic SMCs were serum-starved for 72 hours, fixed, and visualized. Upper images represent no Cy2 control, while the lower images represents basal ascending Id3 abundance after serum starvation. SMCs were stained for nuclei (Hoechst, blue), Id3 (green, right column only), and α -SMC actin (red). Merged images are in the bottom panels with Id3 and α -SMC actin colocalization represented by yellow.

Online Figure X



Online Figure X. AngII-induced nuclei localization of Id3 in SMCs harvested from ascending aortas. Ascending aortic SMCs were serum-starved for 72 hours and incubated with AngII (1 μ M) for 1 (upper images), 12 (middle images), or 24 (lower images) hours. SMCs were stained for nuclei (Hoechst, blue), Id3 (green), and α -SMC actin (red). Images were merged, with Id3 and nuclei colocalization represented by pale blue and Id3 and α -SMC actin colocalization represented by yellow.

Online Figure XI



Online Figure XI. Id3 is minimally expressed in thoracic and abdominal SMCs. Thoracic (upper images), suprarenal (middle images), and infrarenal (lower images) aortic SMCs were serum-starved for 72 hours and incubated with AngII for 24 hours. SMCs were stained for nuclei (Hoechst, blue), Id3 (green), and α -SMC actin (red). Merged images are represented in the bottom panels, with Id3 and α -SMC actin colocalization represented by yellow.

Online Table I. Body weight, plasma renin concentrations, and medial area.

Mouse Strain	Infusions	Body Weight (g)	Plasma Renin Concentration (ng/ml/30min)	Aorta Medial Area (mm ²)			
				Ascending	Thoracic	Suprarenal	Infrarenal
C57BL/6	saline	22.0 ± 0.4	9.6 ± 1.8*	0.105 ± 0.007	0.0775 ± 0.005	0.0559 ± 0.002	0.0390 ± 0.002
	AngII	24.4 ± 0.6	1.2 ± 0.8	0.204 ± 0.020 [†]	0.129 ± 0.009 [†]	0.101 ± 0.005 [†]	0.0682 ± 0.005 [†]
	NE	23.7 ± 0.7	12.3 ± 1.1*	0.120 ± 0.020	0.0737 ± 0.002	0.0590 ± 0.005	0.0381 ± 0.001
AT1aR ^{-/-}	saline	26.8 ± 0.5	45.2 ± 2.5*	0.126 ± 0.009	0.0702 ± 0.002	0.0570 ± 0.003	0.0353 ± 0.001
	AngII	25.6 ± 0.3	24.8 ± 3.3	0.126 ± 0.006	0.0649 ± 0.004	0.0551 ± 0.005	0.0319 ± 0.001
	NE	26.4 ± 0.3	50.8 ± 3.2*	0.137 ± 0.009	0.0704 ± 0.008	0.0600 ± 0.008	0.0332 ± 0.001
	losartan	32.4 ± 0.6	50.7 ± 11.2*	ND	ND	ND	ND
	AngII + losartan	30.8 ± 1.0	48.0 ± 6.5*	ND	ND	ND	ND
C57 ^{p47/p47}	saline	26.6 ± 0.4	12.6 ± 0.5*	0.128 ± 0.008	0.0689 ± 0.002	0.0623 ± 0.002	0.0351 ± 0.001
	AngII	26.9 ± 0.9	3.0 ± 0.6	0.129 ± 0.010	0.0746 ± 0.006	0.0683 ± 0.003	0.0361 ± 0.002
	NE	26.8 ± 0.5	14.7 ± 2.1*	0.133 ± 0.040	0.0675 ± 0.002	0.0589 ± 0.002	0.0349 ± 0.002
ld3 ^{-/-}	saline	27.8 ± 0.6	14.9 ± 3.6**	0.137 ± 0.003	ND	0.0562 ± 0.002	ND
	AngII	28.3 ± 1.1	2.1 ± 0.2	0.244 ± 0.020 [†]	ND	0.118 ± 0.008 [†]	ND

Values are represented as mean ± SEM. ND: not determined.

* Denotes P<0.004 for comparisons to unmarked categories within mouse strains.

[†] Denotes P<0.001 in AngII vs all other groups within mouse strains.

All tests were performed using One-Way ANOVA with post hoc analysis performed using Holm-Sidak.